

A dual-reciprocity boundary element method for axisymmetric thermoelastostatic analysis of nonhomogeneous materials

B. I. Yun* and W. T. Ang
Division of Engineering Mechanics
School of Mechanical and Aerospace Engineering
Nanyang Technological University
Singapore 639798

Abstract

The problem of determining the axisymmetric time independent temperature and thermoelastic displacement and stress fields in a non-homogeneous material is solved numerically by using a dual-reciprocity boundary element technique. Interpolating functions that are bounded in the solution domain but that are in relatively simple elementary forms for easy computation are constructed for treating the domain integrals in the dual-reciprocity boundary element formulation. The proposed numerical approach is successfully applied to solve several specific problems.

This is the preprint of an article accepted for publication in *Engineering Analysis with Boundary Elements*. The article will be in press very soon. Once it is in press, its bibliographic details (year of publication, volume and page numbers) may be obtained through the link <http://dx.doi.org/j.enganabound.2012.06.008> (to be activated soon).
Status as at 14 July 2012.

* Author for correspondence (B. I. Yun)
E-mail: YUNB0003@e.ntu.edu.sg

1 Introduction

The axisymmetric analysis of solids with material properties that vary continuously from point to point in space has recently attracted the attention of many researchers. To mention a few examples, Chaudhuri and Ray [8] and Clements and Kusuma [9] had used integral transform techniques to analyze axisymmetric indentations of anisotropic half-spaces with particular functionally graded elastic moduli; Ochiai, Sladek and Sladek [14] had devised a boundary element method for the numerical solution of an axisymmetric elastic problem involving nonhomogeneous bodies; and Theotokoglou and Stampouloglou [18] had derived exact solutions for axisymmetric deformations of radially graded cylinders.

During the last few decades, the boundary element methods have been used to solve a wide range of problems in physical and engineering sciences – see, for example, Ang and Clements [2] (stress analysis in an anisotropic body), Brebbia and Dominguez [5] (potential problems), Liang and Subramaniam [12] (electrostatic analysis in molecular biology), Mammoli and Ingber [13] (fluid flow) and Rizzo [16] (elastostatic analysis in isotropic elasticity). If the problem under consideration is governed by a homogeneous elliptic partial differential equation with constant coefficients (or a system of such equations), a boundary integral equation (or a system of boundary integral equations) may be derived to obtain a boundary element solution for the problem. The boundary integral equation, even in its discretized form, is in effect an exact solution of the governing partial differential equation. This explains why the boundary element solution may still be accurate even if rather crude approximations such as constant boundary elements are used. Another advantage of the boundary element solution is that only the boundary of the solution has to be discretized into elements. For an axisymmetric

problem, the boundary is a curve and can be easily discretized by placing closely packed points on the curve and joining up two consecutive neighboring points to form straight line elements.

Among the earliest works on axisymmetric boundary element methods are Cruse, Snow and Wilson [10] and Wrobel and Brebbia [20]. The boundary integral formulations for axisymmetric deformations and heat conduction in homogeneous isotropic bodies as given in [10] and [20] respectively are obtained by integrating axially the corresponding three-dimensional boundary integral equations. The kernels of the axisymmetric boundary integral equations are expressed in terms of complete elliptic integrals of the first and second kind. Such a boundary element approach has been extended to solve axisymmetric elastodynamic and thermoelastic problems involving homogeneous isotropic bodies, such as in Dargush and Banerjee [11], Rudolphi [17] and Wang and Banerjee [19]. In some cases, domain integrals may be present in the axisymmetric boundary element formulations for elastodynamics and thermoelasticity. Various approaches, such as the method of particular integrals (as in Park [15]) and dual-reciprocity method (Agnantiaris, Polyzos and Beskos [1]), have been used to treat the domain integrals.

In the current work here, a dual-reciprocity boundary element method is proposed for determining the axisymmetric thermoelastostatic fields in a nonhomogeneous isotropic body. The thermal conductivity, shear modulus and stress-temperature coefficients are functionally graded along the axial and radial directions of the axisymmetric body, while the Poisson's ratio is constant. An integral formulation of the problem under consideration is derived by using the fundamental solution for the partial differential equations governing the axisymmetric elastostatic deformation of a homogeneous body. In addition to the usual boundary integrals over a curve on the axisymmetric

plane, the formulation contains domain integrals due to continuously varying material properties and thermal effects. The domain integrals can be expressed in terms of boundary integrals using the dual-reciprocity method pioneered by Brebbia and Nardini [6]. For the dual-reciprocity method, interpolating functions that are bounded in the solution domain but that are in relatively simple elementary forms for easy computation are introduced here. The dual-reciprocity boundary element approach here is successfully applied to solve several axisymmetric thermoelastostatic problems for specific variations of the thermal conductivity, shear modulus and stress-temperature coefficients.

2 Statement of problem

The region Ω in Figure 1 is rotated by an angle of 360° about the z axis to form a three-dimensional solid. The boundary of the solid is the surface generated by rotating the curve Γ . Note that the coordinate r gives the distance of a point from the z axis.

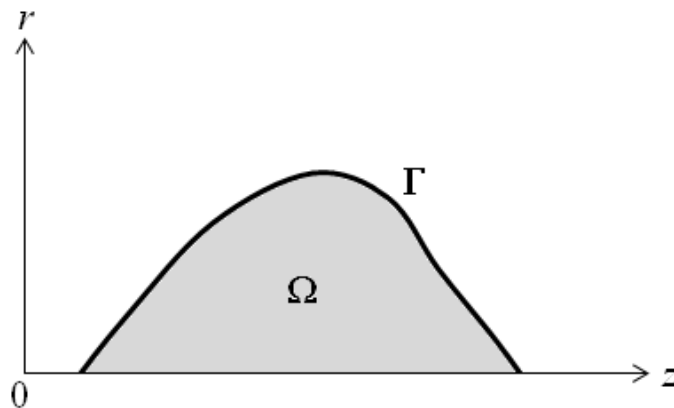


Figure 1. A geometrical sketch of the problem.

The material in the solid is isotropic and nonhomogeneous with its thermal conductivity κ , shear modulus μ and stress-temperature coefficient β functionally graded, that is, κ , μ and β are positive smoothly varying functions of r and z in Ω . The Poisson's ratio ν of the material is a constant such that $-1 < \nu < 1/2$.

The thermoelastic fields in the solid are independent of time and vary with only the spatial coordinates r and z . Furthermore, in the cylindrical polar coordinates r , θ and z , the only non-zero components of the displacement are u_r and u_z , and the non-zero stress components are σ_{rr} , σ_{rz} , $\sigma_{\theta\theta}$ and σ_{zz} . The components of the axisymmetric thermoelastic traction are $t_r = \sigma_{rr}n_r + \sigma_{rz}n_z$ and $t_z = \sigma_{rz}n_r + \sigma_{zz}n_z$, where n_r and n_z are respectively the r and z components of the unit outward normal vector to Γ .

At each point on Γ , either the temperature or the normal heat flux which may be expressed as a linear function of the unknown boundary temperature and any two of the four components u_r , u_z , t_r and t_z are suitably specified. The problem is to determine the thermoelastostatic fields throughout the solid.

3 Basic equations of thermoelastostatics

The steady state axisymmetric temperature $T(r, z)$ in a homogeneous isotropic body is governed by

$$\kappa \nabla_{\text{axis}}^2 T + \frac{\partial \kappa}{\partial r} \frac{\partial T}{\partial r} + \frac{\partial \kappa}{\partial z} \frac{\partial T}{\partial z} = -Q, \quad (1)$$

where Q is the internal heat generation term and ∇_{axis}^2 is the axisymmetric Laplacian operator defined by

$$\nabla_{\text{axis}}^2 \stackrel{\text{def}}{=} \frac{\partial^2}{\partial r^2} + \frac{1}{r} \frac{\partial}{\partial r} + \frac{\partial^2}{\partial z^2}. \quad (2)$$

The static axisymmetric stress components σ_{rr} , σ_{rz} , σ_{zz} and $\sigma_{\theta\theta}$ satisfy

$$\begin{aligned}\frac{\partial\sigma_{rr}}{\partial r} + \frac{\partial\sigma_{rz}}{\partial z} + \frac{\sigma_{rr} - \sigma_{\theta\theta}}{r} &= -F_r, \\ \frac{\partial\sigma_{rz}}{\partial r} + \frac{\partial\sigma_{zz}}{\partial z} + \frac{\sigma_{rz}}{r} &= -F_z,\end{aligned}\quad (3)$$

where F_r and F_z are respectively the r and z components of the body force.

The constitutive equations for thermoelasticity are

$$\begin{aligned}\sigma_{rr} &= 2\mu\left(\frac{\partial u_r}{\partial r} + \frac{\nu}{1-2\nu}\left[\frac{\partial u_r}{\partial r} + \frac{u_r}{r} + \frac{\partial u_z}{\partial z}\right]\right) - \beta(T - T_0), \\ \sigma_{zz} &= 2\mu\left(\frac{\partial u_z}{\partial z} + \frac{\nu}{1-2\nu}\left[\frac{\partial u_r}{\partial r} + \frac{u_r}{r} + \frac{\partial u_z}{\partial z}\right]\right) - \beta(T - T_0), \\ \sigma_{\theta\theta} &= 2\mu\left(\frac{u_r}{r} + \frac{\nu}{1-2\nu}\left[\frac{\partial u_r}{\partial r} + \frac{u_r}{r} + \frac{\partial u_z}{\partial z}\right]\right) - \beta(T - T_0), \\ \sigma_{rz} &= \mu\left(\frac{\partial u_r}{\partial z} + \frac{\partial u_z}{\partial r}\right),\end{aligned}\quad (4)$$

where T_0 is a constant reference temperature at which the body does not experience any thermally induced stress.

Use of (3) and (4) gives

$$\begin{aligned}&\nabla_{\text{axis}}^2 u_r - \frac{u_r}{r^2} + \frac{1}{1-2\nu}\frac{\partial}{\partial r}\left(\frac{\partial u_r}{\partial r} + \frac{u_r}{r} + \frac{\partial u_z}{\partial z}\right) \\ &= \frac{1}{\mu}\left\{\beta\frac{\partial T}{\partial r} + \frac{\partial\beta}{\partial r}(T - T_0) - F_r - \frac{\partial\mu}{\partial z}\left(\frac{\partial u_r}{\partial z} + \frac{\partial u_z}{\partial r}\right) - 2\frac{\partial\mu}{\partial r}\left[\frac{\partial u_r}{\partial r} + \frac{\nu}{1-2\nu}\left(\frac{\partial u_r}{\partial r} + \frac{u_r}{r} + \frac{\partial u_z}{\partial z}\right)\right]\right\}, \\ &\nabla_{\text{axis}}^2 u_z + \frac{1}{1-2\nu}\frac{\partial}{\partial z}\left(\frac{\partial u_r}{\partial r} + \frac{u_r}{r} + \frac{\partial u_z}{\partial z}\right) \\ &= \frac{1}{\mu}\left\{\beta\frac{\partial T}{\partial z} + \frac{\partial\beta}{\partial z}(T - T_0) - F_z - \frac{\partial\mu}{\partial r}\left(\frac{\partial u_r}{\partial z} + \frac{\partial u_z}{\partial r}\right) - 2\frac{\partial\mu}{\partial z}\left[\frac{\partial u_z}{\partial z} + \frac{\nu}{1-2\nu}\left(\frac{\partial u_r}{\partial r} + \frac{u_r}{r} + \frac{\partial u_z}{\partial z}\right)\right]\right\},\end{aligned}\quad (5)$$

The problem stated in Section 2 requires (1) and (5) to be solved in Ω subject to the boundary conditions specified on Γ .

4 Integral equations

4.1 Heat conduction

The governing partial differential equation (1) may be rewritten as

$$\nabla_{\text{axis}}^2(\sqrt{\kappa}T) = -\frac{Q}{\sqrt{\kappa}} + T \cdot \nabla^2(\sqrt{\kappa}). \quad (6)$$

Following the analysis in Brebbia, Telles and Wrobel [7]), we can recast (6) into the integral equation

$$\begin{aligned} & \gamma(\underline{\mathbf{x}}_0)\sqrt{\kappa(\underline{\mathbf{x}}_0)}T(\underline{\mathbf{x}}_0) \\ &= \int_{\Gamma} \left\{ T(\underline{\mathbf{x}})[\sqrt{\kappa(\underline{\mathbf{x}})}G_1(\underline{\mathbf{x}}; \underline{\mathbf{x}}_0; \underline{\mathbf{n}}(\underline{\mathbf{x}})) - \frac{\partial\sqrt{\kappa(\underline{\mathbf{x}})}}{\partial n}G_0(\underline{\mathbf{x}}; \underline{\mathbf{x}}_0)] \right. \\ & \quad \left. - \sqrt{\kappa(\underline{\mathbf{x}})}G_0(\underline{\mathbf{x}}; \underline{\mathbf{x}}_0)q(\underline{\mathbf{x}}; \underline{\mathbf{n}}(\underline{\mathbf{x}})) \right\} r ds(\underline{\mathbf{x}}) \\ & \quad + \iint_{\Omega} G_0(\underline{\mathbf{x}}; \underline{\mathbf{x}}_0) \left[-\frac{Q(\underline{\mathbf{x}})}{\sqrt{\kappa(\underline{\mathbf{x}})}} + T(\underline{\mathbf{x}}) \cdot \nabla^2(\sqrt{\kappa(\underline{\mathbf{x}})}) \right] r dr dz \\ & \quad \text{for } \underline{\mathbf{x}}_0 \in \Omega \cup \Gamma, \end{aligned} \quad (7)$$

where $\underline{\mathbf{x}} = (r, z)$, $\underline{\mathbf{x}}_0 = (r_0, z_0)$, $\gamma(\underline{\mathbf{x}}_0) = 1$ if $\underline{\mathbf{x}}_0$ lies in the interior of Ω , $\gamma(\underline{\mathbf{x}}_0) = 1/2$ if $\underline{\mathbf{x}}_0$ lies on a smooth part of Γ , $ds(\underline{\mathbf{x}})$ denotes the length of an infinitesimal part of the curve Γ , $\underline{\mathbf{n}}(\underline{\mathbf{x}}) = [n_r(\underline{\mathbf{x}}), n_z(\underline{\mathbf{x}})]$ (for $\underline{\mathbf{x}} \in \Gamma$) is the unit normal vector to Γ pointing out of Ω , $G_0(\underline{\mathbf{x}}; \underline{\mathbf{x}}_0)$ and $G_1(\underline{\mathbf{x}}; \underline{\mathbf{x}}_0; \underline{\mathbf{n}}(\underline{\mathbf{x}}))$ are as given in Appendix A and $q(\underline{\mathbf{x}}; \underline{\mathbf{n}}(\underline{\mathbf{x}}))$ is defined by

$$q(\underline{\mathbf{x}}; \underline{\mathbf{n}}(\underline{\mathbf{x}})) = n_r(\underline{\mathbf{x}})\frac{\partial}{\partial r}[T(\underline{\mathbf{x}})] + n_z(\underline{\mathbf{x}})\frac{\partial}{\partial z}[T(\underline{\mathbf{x}})]. \quad (8)$$

4.2 Thermoelastostatics

For convenience here, uppercase Latin subscripts (such as J and K) which are given the values r and z are used to denote axisymmetric components. Furthermore, the Einsteinian convention of summing over a repeated subscript is

adopted. Thus, for example, u_K is used to denote the axisymmetric displacement components u_r and u_z , and $G_{KJ}u_J$ refers to the sums $G_{rr}u_r + G_{rz}u_z$ and $G_{zr}u_r + G_{zz}u_z$.

The integral equations for (5) is given by (see Bakr [4])

$$\begin{aligned}
\gamma(\underline{\mathbf{x}}_0)u_K(\underline{\mathbf{x}}_0) &= \int_{\Gamma} (\Phi_{JK}(\underline{\mathbf{x}}; \underline{\mathbf{x}}_0)p_J(\underline{\mathbf{x}}; \underline{\mathbf{n}}(\underline{\mathbf{x}})) - \Psi_{JK}(\underline{\mathbf{x}}; \underline{\mathbf{x}}_0; \underline{\mathbf{n}}(\underline{\mathbf{x}}))u_J(\underline{\mathbf{x}}))rds(\underline{\mathbf{x}}) \\
&+ \iint_{\Omega} \frac{1}{\mu(\underline{\mathbf{x}})}\Phi_{JK}(\underline{\mathbf{x}}; \underline{\mathbf{x}}_0)\{-\beta(\underline{\mathbf{x}})\frac{\partial}{\partial x_J}[T(\underline{\mathbf{x}})] \\
&\quad - \frac{\partial}{\partial x_J}[\beta(\underline{\mathbf{x}})](T - T_0) + F_J(\underline{\mathbf{x}}) \\
&\quad + \frac{\partial}{\partial x_J}[\mu(\underline{\mathbf{x}})]\frac{2\nu}{(1 - 2\nu)r}u_r(\underline{\mathbf{x}}) \\
&\quad + X_{JN}(\underline{\mathbf{x}})\frac{\partial}{\partial z}[u_N(\underline{\mathbf{x}})] + Y_{JN}(\underline{\mathbf{x}})\frac{\partial}{\partial r}[u_N(\underline{\mathbf{x}})]\}rdrdz \\
&\quad \text{for } \underline{\mathbf{x}}_0 \in \Omega \cup \Gamma, \tag{9}
\end{aligned}$$

where $x_r = r$, $x_z = z$, $\Phi_{JK}(\underline{\mathbf{x}}; \underline{\mathbf{x}}_0)$ and $\Psi_{JK}(\underline{\mathbf{x}}; \underline{\mathbf{x}}_0; \underline{\mathbf{n}}(\underline{\mathbf{x}}))$ are as given in the Appendix B, $p_J(\underline{\mathbf{x}}; \underline{\mathbf{n}}(\underline{\mathbf{x}}))$ are defined by

$$\begin{aligned}
p_r(\underline{\mathbf{x}}; \underline{\mathbf{n}}(\underline{\mathbf{x}})) &= 2\left(\frac{\partial u_r}{\partial r} + \frac{\nu}{1 - 2\nu}\left[\frac{\partial u_r}{\partial r} + \frac{u_r}{r} + \frac{\partial u_z}{\partial z}\right]\right)n_r(\underline{\mathbf{x}}) \\
&\quad + \left(\frac{\partial u_r}{\partial z} + \frac{\partial u_z}{\partial r}\right)n_z(\underline{\mathbf{x}}), \\
p_z(\underline{\mathbf{x}}; \underline{\mathbf{n}}(\underline{\mathbf{x}})) &= \left(\frac{\partial u_r}{\partial z} + \frac{\partial u_z}{\partial r}\right)n_r(\underline{\mathbf{x}}) \\
&\quad + 2\left(\frac{\partial u_z}{\partial z} + \frac{\nu}{1 - 2\nu}\left[\frac{\partial u_r}{\partial r} + \frac{u_r}{r} + \frac{\partial u_z}{\partial z}\right]\right)n_z(\underline{\mathbf{x}}), \tag{10}
\end{aligned}$$

and

$$\begin{aligned}
X_{rr}(\underline{\mathbf{x}}) &= \frac{\partial\mu(\underline{\mathbf{x}})}{\partial z}, \quad X_{rz}(\underline{\mathbf{x}}) = \frac{2\nu}{1-2\nu} \frac{\partial\mu(\underline{\mathbf{x}})}{\partial r}, \\
X_{zr}(\underline{\mathbf{x}}) &= \frac{\partial\mu(\underline{\mathbf{x}})}{\partial r}, \quad X_{zz}(\underline{\mathbf{x}}) = \frac{\partial\mu(\underline{\mathbf{x}})}{\partial z} \frac{2(1-\nu)}{1-2\nu}, \\
Y_{rr}(\underline{\mathbf{x}}) &= \frac{\partial\mu(\underline{\mathbf{x}})}{\partial r} \frac{2(1-\nu)}{1-2\nu}, \quad Y_{rz}(\underline{\mathbf{x}}) = \frac{\partial\mu(\underline{\mathbf{x}})}{\partial z}, \\
Y_{zr}(\underline{\mathbf{x}}) &= \frac{2\nu}{1-2\nu} \frac{\partial\mu(\underline{\mathbf{x}})}{\partial z}, \quad Y_{zz}(\underline{\mathbf{x}}) = \frac{\partial\mu(\underline{\mathbf{x}})}{\partial r}.
\end{aligned} \tag{11}$$

Note that $p_J(\underline{\mathbf{x}}; \underline{\mathbf{n}}(\underline{\mathbf{x}}))$ are related to the axisymmetric components $t_J(\underline{\mathbf{x}}; \underline{\mathbf{n}}(\underline{\mathbf{x}}))$ of the thermoelastic traction by

$$t_J(\underline{\mathbf{x}}; \underline{\mathbf{n}}(\underline{\mathbf{x}})) = \mu(\underline{\mathbf{x}})p_J(\underline{\mathbf{x}}; \underline{\mathbf{n}}(\underline{\mathbf{x}})) - \beta(\underline{\mathbf{x}})[T(\underline{\mathbf{x}}) - T_0]\delta_{JL}n_L(\underline{\mathbf{x}}), \tag{12}$$

where δ_{JN} is the Kronecker-delta defined by $\delta_{rr} = \delta_{zz} = 1$ and $\delta_{rz} = \delta_{zr} = 0$

5 Dual-reciprocity method

In this section, we explain how double integrals over Ω of the form in (7) and (9) can be approximately reduced to line integrals over Γ by using the dual-reciprocity method.

Let $\underline{\mathbf{y}}^{(1)}, \underline{\mathbf{y}}^{(2)}, \dots, \underline{\mathbf{y}}^{(M-1)}$ and $\underline{\mathbf{y}}^{(M)}$ be M selected points which are well spaced out in $\Omega \cup \Gamma$. None of the selected points lies on the z axis.

If $f(\underline{\mathbf{x}})$ is a function that can be approximated using

$$f(\underline{\mathbf{x}}) \simeq \sum_{n=1}^M \alpha^{(n)} \phi(\underline{\mathbf{x}}; \underline{\mathbf{y}}^{(n)}) \text{ for } \underline{\mathbf{x}} \in \Omega, \tag{13}$$

where $\alpha^{(n)}$ are constant coefficients to be determined and $\phi(\underline{\mathbf{x}}; \underline{\mathbf{y}})$ is a local interpolating function which can be written in the form

$$\phi(\underline{\mathbf{x}}; \underline{\mathbf{y}}) = \nabla_{\text{axis}}^2 \chi(\underline{\mathbf{x}}; \underline{\mathbf{y}}), \tag{14}$$

then

$$\iint_{\Omega} G_0(\underline{\mathbf{x}}; \underline{\mathbf{x}}_0) f(\underline{\mathbf{x}}) r dr dz \simeq \sum_{n=1}^M \alpha^{(n)} W^{(n)}(\underline{\mathbf{x}}_0), \quad (15)$$

where

$$\begin{aligned} W^{(n)}(\underline{\mathbf{x}}_0) &= \gamma(\underline{\mathbf{x}}_0) \chi(\underline{\mathbf{x}}_0; \underline{\mathbf{y}}^{(n)}) + \int_{\Gamma} [G_0(\underline{\mathbf{x}}; \underline{\mathbf{x}}_0) \frac{\partial}{\partial n} [\chi(\underline{\mathbf{x}}; \underline{\mathbf{y}}^{(n)})] \\ &\quad - G_1(\underline{\mathbf{x}}; \underline{\mathbf{x}}_0; \underline{\mathbf{n}}(\underline{\mathbf{x}})) \chi(\underline{\mathbf{x}}; \underline{\mathbf{y}}^{(n)})] r ds(\underline{\mathbf{x}}), \\ \frac{\partial}{\partial n} [\chi(\underline{\mathbf{x}}; \underline{\mathbf{y}})] &= n_r(\underline{\mathbf{x}}) \frac{\partial}{\partial r} [\chi(\underline{\mathbf{x}}; \underline{\mathbf{y}})] + n_z(\underline{\mathbf{x}}) \frac{\partial}{\partial z} [\chi(\underline{\mathbf{x}}; \underline{\mathbf{y}})]. \end{aligned} \quad (16)$$

We may let $\underline{\mathbf{x}} = \underline{\mathbf{y}}^{(k)}$ ($k = 1, 2, \dots, M$) in (13) to obtain

$$\sum_{n=1}^M \alpha^{(n)} \phi(\underline{\mathbf{y}}^{(k)}; \underline{\mathbf{y}}^{(n)}) = f(\underline{\mathbf{y}}^{(k)}) \text{ for } k = 1, 2, \dots, M, \quad (17)$$

which may be solved as a system of M linear algebraic equations to find the unknown coefficients $\alpha^{(n)}$.

In Yun and Ang [21], the local interpolating function $\phi(\underline{\mathbf{x}}; \underline{\mathbf{y}})$ is constructed from (14) by letting

$$\chi(\underline{\mathbf{x}}; \underline{\mathbf{y}}) = \frac{1}{9} \{ [\sigma(\underline{\mathbf{x}}; \underline{\mathbf{y}})]^3 + [\sigma(\underline{\mathbf{x}}; -\rho, \zeta)]^3 \}, \quad (18)$$

where $\underline{\mathbf{y}} = (\rho, \zeta)$ and $\sigma(\underline{\mathbf{x}}; \underline{\mathbf{y}}) = \sqrt{(r - \rho)^2 + (z - \zeta)^2}$ ($\underline{\mathbf{x}} = (r, z)$).

The function $\phi(\underline{\mathbf{x}}; \underline{\mathbf{y}})$ corresponding to $\chi(\underline{\mathbf{x}}; \underline{\mathbf{y}})$ in (18) is then given by

$$\phi(\underline{\mathbf{x}}; \underline{\mathbf{y}}) = \left[\frac{4}{3} - \frac{\rho}{3r} \right] \sigma(\underline{\mathbf{x}}; \underline{\mathbf{y}}) + \left[\frac{4}{3} + \frac{\rho}{3r} \right] \sigma(\underline{\mathbf{x}}; -\rho, \zeta). \quad (19)$$

As given by (19), $\phi(\underline{\mathbf{x}}; \underline{\mathbf{y}})$ is bounded at all points (r, z) in the region $r > 0$.

Formula (15) together with (16), (17), (18) and (19) can be used to reduce the double integral over Ω in (7) to line integrals over Γ .

The idea outlined above will be extended to the more complicated double integral in (9).

We use local interpolating functions $\phi_{IJ}(\underline{\mathbf{x}}; \underline{\mathbf{y}})$ that can be expressed in the form

$$\begin{aligned}\phi_{rJ}(\underline{\mathbf{x}}; \underline{\mathbf{y}}) &= \nabla_{\text{axis}}^2 \chi_{rJ}(\underline{\mathbf{x}}; \underline{\mathbf{y}}) - \frac{\chi_{rJ}(\underline{\mathbf{x}}; \underline{\mathbf{y}})}{r^2} \\ &\quad + \frac{1}{1-2\nu} \frac{\partial}{\partial r} \left(\frac{\partial}{\partial r} [\chi_{rJ}(\underline{\mathbf{x}}; \underline{\mathbf{y}})] + \frac{\chi_{rJ}(\underline{\mathbf{x}}; \underline{\mathbf{y}})}{r} + \frac{\partial}{\partial z} [\chi_{zJ}(\underline{\mathbf{x}}; \underline{\mathbf{y}})] \right), \\ \phi_{zJ}(\underline{\mathbf{x}}; \underline{\mathbf{y}}) &= \nabla_{\text{axis}}^2 \chi_{zJ}(\underline{\mathbf{x}}; \underline{\mathbf{y}}) \\ &\quad + \frac{1}{1-2\nu} \frac{\partial}{\partial z} \left(\frac{\partial}{\partial r} [\chi_{rJ}(\underline{\mathbf{x}}; \underline{\mathbf{y}})] + \frac{\chi_{rJ}(\underline{\mathbf{x}}; \underline{\mathbf{y}})}{r} + \frac{\partial}{\partial z} [\chi_{zJ}(\underline{\mathbf{x}}; \underline{\mathbf{y}})] \right).\end{aligned}\tag{20}$$

If the functions $f_J(\underline{\mathbf{x}})$ can be approximated as

$$f_J(\underline{\mathbf{x}}) \simeq \sum_{n=1}^M \phi_{JN}(\underline{\mathbf{x}}; \underline{\mathbf{y}}^{(n)}) \alpha_N^{(n)} \text{ for } \underline{\mathbf{x}} \in \Omega,\tag{21}$$

where $\alpha_N^{(n)}$ are constant coefficients, then

$$\iint_{\Omega} \Phi_{JK}(\underline{\mathbf{x}}; \underline{\mathbf{x}}_0) f_J(\underline{\mathbf{x}}) r dr dz \simeq \sum_{n=1}^M \alpha_N^{(n)} W_{KN}^{(n)}(\underline{\mathbf{x}}_0),\tag{22}$$

where

$$\begin{aligned}W_{KN}^{(n)}(\underline{\mathbf{x}}_0) &= -\gamma(\underline{\mathbf{x}}_0) \chi_{KN}(\underline{\mathbf{x}}_0; \underline{\mathbf{y}}^{(n)}) \\ &\quad + \int_{\Gamma} (\Phi_{JK}(\underline{\mathbf{x}}; \underline{\mathbf{x}}_0) \tau_{JN}(\underline{\mathbf{x}}; \underline{\mathbf{y}}^{(n)}; \underline{\mathbf{n}}(\underline{\mathbf{x}})) \\ &\quad - \Psi_{JK}(\underline{\mathbf{x}}; \underline{\mathbf{x}}_0; \underline{\mathbf{n}}(\underline{\mathbf{x}})) \chi_{JN}(\underline{\mathbf{x}}; \underline{\mathbf{y}}^{(n)})) r ds(\underline{\mathbf{x}}),\end{aligned}\tag{23}$$

and

$$\begin{aligned}
\tau_{rN}(\underline{\mathbf{x}}; \underline{\mathbf{y}}; \underline{\mathbf{n}}(\underline{\mathbf{x}})) &= 2n_r(\underline{\mathbf{x}}) \left\{ \frac{\partial}{\partial r} [\chi_{rN}(\underline{\mathbf{x}}; \underline{\mathbf{y}})] + \frac{\nu}{1-2\nu} \left(\frac{\partial}{\partial r} [\chi_{rN}(\underline{\mathbf{x}}; \underline{\mathbf{y}})] \right. \right. \\
&\quad \left. \left. + \frac{\chi_{rN}(\underline{\mathbf{x}}; \underline{\mathbf{y}})}{r} + \frac{\partial}{\partial z} [\chi_{zN}(\underline{\mathbf{x}}; \underline{\mathbf{y}})] \right) \right\} \\
&\quad + n_z(\underline{\mathbf{x}}) \left\{ \frac{\partial}{\partial z} [\chi_{rN}(\underline{\mathbf{x}}; \underline{\mathbf{y}})] + \frac{\partial}{\partial r} [\chi_{zN}(\underline{\mathbf{x}}; \underline{\mathbf{y}})] \right\}, \\
\tau_{zN}(\underline{\mathbf{x}}; \underline{\mathbf{y}}; \underline{\mathbf{n}}(\underline{\mathbf{x}})) &= n_r(\underline{\mathbf{x}}) \left\{ \frac{\partial}{\partial z} [\chi_{rN}(\underline{\mathbf{x}}; \underline{\mathbf{y}})] + \frac{\partial}{\partial r} [\chi_{zN}(\underline{\mathbf{x}}; \underline{\mathbf{y}})] \right\} \\
&\quad + 2n_z(\underline{\mathbf{x}}) \left\{ \frac{\partial}{\partial z} [\chi_{zN}(\underline{\mathbf{x}}; \underline{\mathbf{y}})] + \frac{\nu}{1-2\nu} \left(\frac{\partial}{\partial r} [\chi_{rN}(\underline{\mathbf{x}}; \underline{\mathbf{y}})] \right. \right. \\
&\quad \left. \left. + \frac{\chi_{rN}(\underline{\mathbf{x}}; \underline{\mathbf{y}})}{r} + \frac{\partial}{\partial z} [\chi_{zN}(\underline{\mathbf{x}}; \underline{\mathbf{y}})] \right) \right\}. \tag{24}
\end{aligned}$$

To construct functions $\phi_{IJ}(\underline{\mathbf{x}}; \underline{\mathbf{y}})$ that are bounded at all points (r, z) for $r > 0$, we take

$$\begin{aligned}
\chi_{rr}(\underline{\mathbf{x}}; \underline{\mathbf{y}}) &= \chi(\underline{\mathbf{x}}; \underline{\mathbf{y}}) - \frac{2}{9} [\sigma(0, z; \underline{\mathbf{y}})]^3, \\
\chi_{zr}(\underline{\mathbf{x}}; \underline{\mathbf{y}}) &= \chi_{rz}(\underline{\mathbf{x}}; \underline{\mathbf{y}}) = 0, \\
\chi_{zz}(\underline{\mathbf{x}}; \underline{\mathbf{y}}) &= \chi(\underline{\mathbf{x}}; \underline{\mathbf{y}}), \tag{25}
\end{aligned}$$

where $\chi(\underline{\mathbf{x}}; \underline{\mathbf{y}})$ is as defined by (21).

The functions $\phi_{IJ}(\underline{\mathbf{x}}; \underline{\mathbf{y}})$ and $\tau_{IJ}(\underline{\mathbf{x}}; \underline{\mathbf{y}}; \underline{\mathbf{n}}(\underline{\mathbf{x}}))$ constructed using (20), (24) and (25) are given in Appendix C. With $\chi_{KN}(\underline{\mathbf{x}}; \underline{\mathbf{y}})$ as given in (25), $\phi_{IJ}(\underline{\mathbf{x}}; \underline{\mathbf{y}})$ can be shown to be bounded at all points (r, z) in the region $r > 0$. In Agnantiaris, Polyzos and Beskos [1], bounded interpolating functions are constructed by integrating axially the corresponding interpolating functions for the three-dimensional dual-reciprocity boundary element method. Explicit expressions for the interpolating functions constructed from the axial integration are, however, very complicated compared to those given in Appendix C. In [1], it appears that the integrals from the axial integration are computed numerically.

We collocate (21) by taking $\underline{\mathbf{x}} = \underline{\mathbf{y}}^{(k)}$ ($k = 1, 2, \dots, M$) to obtain

$$\sum_{n=1}^M \phi_{JN}(\underline{\mathbf{y}}^{(k)}; \underline{\mathbf{y}}^{(n)}) \alpha_N^{(n)} = f_J(\underline{\mathbf{y}}^{(k)}) \text{ for } k = 1, 2, \dots, M. \quad (26)$$

The coefficients $\alpha_N^{(n)}$ can then be obtained in terms of $f_J(\underline{\mathbf{y}}^{(k)})$ by inverting (26).

6 Boundary element solution

The integral equations in (7) and (9) are used here to solve the problem in Section 2.

The curve Γ is discretized into N straight line elements denoted by $\Gamma^{(1)}$, $\Gamma^{(2)}$, \dots , $\Gamma^{(N-1)}$ and $\Gamma^{(N)}$. Over $\Gamma^{(k)}$, the functions T , q , u_J and p_J are approximated as constants $T^{(k)}$, $q^{(k)}$, $u_J^{(k)}$ and $p_J^{(k)}$ respectively. For collocation points, take $\underline{\mathbf{y}}^{(1)}$, $\underline{\mathbf{y}}^{(2)}$, \dots , $\underline{\mathbf{y}}^{(N-1)}$ and $\underline{\mathbf{y}}^{(N)}$ to be the midpoints of $\Gamma^{(1)}$, $\Gamma^{(2)}$, \dots , $\Gamma^{(N-1)}$ and $\Gamma^{(N)}$ respectively, and $\underline{\mathbf{y}}^{(N+1)}$, $\underline{\mathbf{y}}^{(N+2)}$, \dots , $\underline{\mathbf{y}}^{(N+L-1)}$ and $\underline{\mathbf{y}}^{(N+L)}$ to be L selected points that are well spaced out in the interior of the region Ω . None of the collocation points lies on the z axis.

With the above and the dual-reciprocity formula in (15), (7) can now be used to obtain

$$\begin{aligned} & \gamma(\underline{\mathbf{y}}^{(m)}) \sqrt{\kappa(\underline{\mathbf{y}}^{(m)})} T^{(m)} \\ &= \sum_{k=1}^N T^{(k)} \int_{\Gamma^{(k)}} [\sqrt{\kappa(\underline{\mathbf{x}})} G_1(\underline{\mathbf{x}}; \underline{\mathbf{y}}^{(m)}; \underline{\mathbf{n}}(\underline{\mathbf{x}})) - \frac{\partial \kappa(\underline{\mathbf{x}})}{\partial n} G_0(\underline{\mathbf{x}}; \underline{\mathbf{y}}^{(m)})] r ds(\underline{\mathbf{x}}) \\ & - \sum_{k=1}^N q^{(k)} \int_{\Gamma^{(k)}} \sqrt{\kappa(\underline{\mathbf{x}})} G_0(\underline{\mathbf{x}}; \underline{\mathbf{y}}^{(m)}) r ds(\underline{\mathbf{x}}) + \sum_{n=1}^{N+L} \alpha^{(n)} W^{(n)}(\underline{\mathbf{y}}^{(m)}) \\ & \text{for } m = 1, 2, \dots, N + L, \end{aligned} \quad (27)$$

and

$$\sum_{n=1}^{N+L} \alpha^{(n)} \phi(\underline{\mathbf{y}}^{(k)}; \underline{\mathbf{y}}^{(n)}) = -\frac{Q(\underline{\mathbf{y}}^{(k)})}{\sqrt{\kappa(\underline{\mathbf{y}}^{(k)})}} + T^{(k)} \cdot \nabla^2(\sqrt{\kappa(\underline{\mathbf{x}})}) \Big|_{\underline{\mathbf{x}}=\underline{\mathbf{y}}^{(k)}} \\ \text{for } k = 1, 2, \dots, N+L, \quad (28)$$

where $\underline{\mathbf{y}}^{(m)} = (\rho^{(m)}, \zeta^{(m)})$.

We can treat (27) and (28) as a system of $2(N+L)$ linear algebraic equations. The $2(N+L)$ unknowns in the system are $\alpha^{(n)}$ for $n = 1, 2, \dots, N+L$, $T^{(p)}$ for $p = N+1, N+2, \dots, N+L$, and either $T^{(k)}$ or $q^{(k)}$ for $k = 1, 2, \dots, N$ (depending on the boundary conditions of the problem).

Similarly, (9) gives

$$\gamma(\underline{\mathbf{y}}^{(m)}) u_K^{(m)} = \sum_{n=1}^{N+L} \alpha_N^{(n)} W_{KN}^{(n)}(\underline{\mathbf{y}}^{(m)}) + \sum_{k=1}^N p_J^{(k)} \int_{\Gamma^{(k)}} \Phi_{JK}(\underline{\mathbf{x}}; \underline{\mathbf{y}}^{(m)}) r ds(\underline{\mathbf{x}}) \\ - \sum_{k=1}^N u_J^{(k)} \int_{\Gamma^{(k)}} \Psi_{JK}(\underline{\mathbf{x}}; \underline{\mathbf{y}}^{(m)}; \underline{\mathbf{n}}(\underline{\mathbf{x}})) r ds(\underline{\mathbf{x}}) \\ \text{for } m = 1, 2, \dots, N+L, \quad (29)$$

and

$$\sum_{n=1}^{N+L} \phi_{JN}(\underline{\mathbf{y}}^{(k)}; \underline{\mathbf{y}}^{(n)}) \alpha_N^{(n)} \\ = \frac{1}{\mu(\underline{\mathbf{y}}^{(k)})} \left\{ -\beta(\underline{\mathbf{y}}^{(k)}) \frac{\partial}{\partial x_J} [T(\underline{\mathbf{x}})] \Big|_{\underline{\mathbf{x}}=\underline{\mathbf{y}}^{(k)}} - \frac{\partial}{\partial x_J} [\beta(\underline{\mathbf{x}})] \Big|_{\underline{\mathbf{x}}=\underline{\mathbf{y}}^{(k)}} (T^{(k)} - T_0) \right. \\ \left. + F_J(\underline{\mathbf{y}}^{(k)}) + \frac{\partial}{\partial x_J} [\mu(\underline{\mathbf{x}})] \Big|_{\underline{\mathbf{x}}=\underline{\mathbf{y}}^{(k)}} \frac{2\nu}{(1-2\nu)r^{(k)}} u_r^{(k)} \right. \\ \left. + X_{JN}(\underline{\mathbf{y}}^{(k)}) \frac{\partial}{\partial z} [u_N(\underline{\mathbf{x}})] \Big|_{\underline{\mathbf{x}}=\underline{\mathbf{y}}^{(k)}} + Y_{JN}(\underline{\mathbf{y}}^{(k)}) \frac{\partial}{\partial r} [u_N(\underline{\mathbf{x}})] \Big|_{\underline{\mathbf{x}}=\underline{\mathbf{y}}^{(k)}} \right\} \\ \text{for } k = 1, 2, \dots, N+L. \quad (30)$$

Unlike (28), the right hand side of (30) contains values of the first order partial derivatives of the unknown functions. To approximate those values, let

$$\begin{aligned}
T(\underline{\mathbf{x}}) &\simeq \sum_{m=1}^{N+L} t^{(m)} \chi(\underline{\mathbf{x}}; \underline{\mathbf{y}}^{(m)}), \\
u_r(\underline{\mathbf{x}}) &\simeq \sum_{m=1}^{N+L} v_r^{(m)} \bar{\chi}(\underline{\mathbf{x}}; \underline{\mathbf{y}}^{(m)}), \\
u_z(\underline{\mathbf{x}}) &\simeq \sum_{m=1}^{N+L} v_z^{(m)} \chi(\underline{\mathbf{x}}; \underline{\mathbf{y}}^{(m)}),
\end{aligned} \tag{31}$$

where $\chi(\underline{\mathbf{x}}; \underline{\mathbf{y}})$ is as defined in (18) and $\bar{\chi}(\underline{\mathbf{x}}; \underline{\mathbf{y}})$ by

$$\bar{\chi}(\underline{\mathbf{x}}; \underline{\mathbf{y}}) = \frac{1}{9} \{[\sigma(\underline{\mathbf{x}}; \underline{\mathbf{y}})]^3 - [\sigma(\underline{\mathbf{x}}; -\rho, \zeta)]^3\}. \tag{32}$$

If we collocate (31) by letting $\underline{\mathbf{x}} = \underline{\mathbf{y}}^{(k)}$ for $k = 1, 2, \dots, N + L$ and invert the resulting equations to determine the constant coefficients $t^{(m)}$ and $v_N^{(m)}$, we obtain

$$\begin{aligned}
\frac{\partial}{\partial x_J} [T(\underline{\mathbf{x}})] &= \sum_{p=1}^{N+L} T^{(p)} \varphi_J^{(p)}(\underline{\mathbf{x}}), \\
\frac{\partial}{\partial x_J} [u_r(\underline{\mathbf{x}})] &= \sum_{p=1}^{N+L} u_r^{(p)} \bar{\varphi}_J^{(p)}(\underline{\mathbf{x}}), \\
\frac{\partial}{\partial x_J} [u_z(\underline{\mathbf{x}})] &= \sum_{p=1}^{N+L} u_z^{(p)} \varphi_J^{(p)}(\underline{\mathbf{x}}),
\end{aligned} \tag{33}$$

where

$$\begin{aligned}
\varphi_J^{(p)}(\underline{\mathbf{x}}) &= \sum_{m=1}^{N+L} \omega^{(mp)} \frac{\partial}{\partial x_J} [\chi(\underline{\mathbf{x}}; \underline{\mathbf{y}}^{(m)})], \\
\bar{\varphi}_J^{(p)}(\underline{\mathbf{x}}) &= \sum_{m=1}^{N+L} \bar{\omega}^{(mp)} \frac{\partial}{\partial x_J} [\bar{\chi}(\underline{\mathbf{x}}; \underline{\mathbf{y}}^{(m)})],
\end{aligned}$$

$$\begin{aligned}
\sum_{m=1}^{N+L} \chi(\underline{\mathbf{x}}^{(k)}; \underline{\mathbf{y}}^{(m)}) \omega^{(mp)} &= \begin{cases} 1 & \text{if } k = p, \\ 0 & \text{if } k \neq p, \end{cases} \\
\sum_{m=1}^{N+L} \bar{\chi}(\underline{\mathbf{x}}^{(k)}; \underline{\mathbf{y}}^{(m)}) \bar{\omega}^{(mp)} &= \begin{cases} 1 & \text{if } k = p, \\ 0 & \text{if } k \neq p. \end{cases}
\end{aligned} \tag{34}$$

It follows that (30) becomes

$$\begin{aligned}
& \sum_{n=1}^M \phi_{JN}(\underline{\mathbf{y}}^{(k)}; \underline{\mathbf{y}}^{(n)}) \alpha_N^{(n)} \\
= & \frac{1}{\mu(\underline{\mathbf{y}}^{(k)})} \left\{ -\beta(\underline{\mathbf{y}}^{(k)}) \sum_{p=1}^{N+L} T^{(p)} \varphi_J^{(p)}(\underline{\mathbf{y}}^{(k)}) - \frac{\partial}{\partial x_J} [\beta(\underline{\mathbf{x}})] \Big|_{\underline{\mathbf{x}}=\underline{\mathbf{y}}^{(k)}} (T^{(k)} - T_0) \right. \\
& + F_J(\underline{\mathbf{y}}^{(k)}) + \frac{\partial}{\partial x_J} [\mu(\underline{\mathbf{x}})] \Big|_{\underline{\mathbf{x}}=\underline{\mathbf{y}}^{(k)}} \frac{2\nu}{(1-2\nu)r} u_r^{(k)} \\
& + \sum_{p=1}^{N+L} [X_{Jr}(\underline{\mathbf{y}}^{(k)}) u_r^{(p)} \bar{\varphi}_z^{(p)}(\underline{\mathbf{y}}^{(k)}) + X_{Jz}(\underline{\mathbf{y}}^{(k)}) u_z^{(p)} \varphi_z^{(p)}(\underline{\mathbf{y}}^{(k)})] \\
& \left. + \sum_{p=1}^{N+L} [Y_{Jr}(\underline{\mathbf{y}}^{(k)}) u_r^{(p)} \bar{\varphi}_r^{(p)}(\underline{\mathbf{y}}^{(k)}) + Y_{Jz}(\underline{\mathbf{y}}^{(k)}) u_z^{(p)} \varphi_r^{(p)}(\underline{\mathbf{y}}^{(k)})] \right\} \\
& \text{for } k = 1, 2, \dots, N+L.
\end{aligned} \tag{35}$$

In (18) and (32), $u_r(\underline{\mathbf{x}})$ and the first order partial derivatives of $T(\underline{\mathbf{x}})$ and $u_z(\underline{\mathbf{x}})$ with respect to r behave as $O(r)$ for small r . Such behaviors are expected of the temperature $T(\underline{\mathbf{x}})$ and the displacement components $u_r(\underline{\mathbf{x}})$ and $u_z(\underline{\mathbf{x}})$ if the solution domain contains points (r, z) where r can be zero.

With $T^{(p)}$ determined from (27) and (28), we may now solve (29) and (35) as a system of $4(N+L)$ linear algebraic equations in $4(N+L)$ unknowns. The unknowns are $\alpha_J^{(n)}$ ($n = 1, 2, \dots, N+L$), two unknowns from the four boundary components $u_r^{(k)}$, $u_z^{(k)}$, $p_r^{(k)}$ and $p_z^{(k)}$ ($k = 1, 2, \dots, N$) and the unknown displacement components $u_K^{(i)}$ ($i = N+1, N+2, \dots, N+L$) at interior collocation points.

7 Specific problems

In this section, the boundary element method outlined in Section 6 is applied to solve some specific problems.

Problem 1. For a particular test problem, take the solution domain as $0 < r < 1$, $0 < z < 1$. The thermal conductivity κ , the stress-temperature coefficient β , the shear modulus μ , the Poisson's ratio ν and the reference temperature T_0 are taken to be given by $\kappa = (r^2 + z + 1)^2$, $\beta = z^2 + 1$, $\mu = r^2 + 1$, $\nu = 0.3$ and $T_0 = 0$ respectively. The internal heat generation Q and body force terms F_r and F_z are given by

$$\begin{aligned} Q(r, z) &= (r^2 + z + 1)(12z^2 + 6r^2z - 6z - 36r^2 - 12), \\ F_r(r, z) &= -2r^3 - 4rz^2 - 38r, \\ F_z(r, z) &= -5z^4 - 8r^2z - 3z^2 - 10z + 16r^2 + 8. \end{aligned}$$

The boundary conditions are taken to be given by

$$\left. \begin{aligned} T(r, 0) &= 3r^2 \\ u_r(r, 0) &= 3r \\ u_z(r, 0) &= -2r^2 \end{aligned} \right\} \text{ for } 0 < r < 1,$$

$$\left. \begin{aligned} \frac{\partial T}{\partial z} \Big|_{z=1} &= -3 \\ u_r(r, 1) &= 4r \\ u_z(r, 1) &= 4 - 2r^2 \end{aligned} \right\} \text{ for } 0 < r < 1,$$

$$\left. \begin{aligned} T(1, z) &= 3 - z^3 \\ u_r(1, z) &= 3 + z^2 \\ u_z(1, z) &= 4z - 2 \end{aligned} \right\} \text{ for } 0 < z < 1.$$

To obtain some numerical results, the boundary is discretized into N equal length elements and L evenly distributed collocation points are chosen

inside the domain. The numerical results are obtained with three different sets of N and L : $(N, L) = (30, 9)$ (Set A), $(N, L) = (90, 121)$ (Set B) and $(N, L) = (270, 361)$ (Set C).

Table 1. A comparison of the numerical and exact values of T at selected interior points.

(r, z)	Set A	Set B	Set C	Exact
(0.25, 0.25)	0.193720	0.173006	0.172138	0.171875
(0.50, 0.25)	0.745310	0.735069	0.734542	0.734375
(0.75, 0.25)	1.672804	1.671976	1.671919	1.671875
(0.25, 0.50)	0.090651	0.064348	0.062965	0.062500
(0.50, 0.50)	0.640126	0.626256	0.625321	0.625000
(0.75, 0.50)	1.565350	1.562901	1.562625	1.562500
(0.25, 0.75)	-0.195026	-0.231369	-0.233598	-0.234375
(0.50, 0.75)	0.354515	0.330494	0.328720	0.328125
(0.75, 0.75)	1.278146	1.267007	1.265953	1.265625

Table 2. A comparison of the numerical and exact values of u_r at selected interior points.

(r, z)	Set A	Set B	Set C	Exact
(0.25, 0.25)	0.766878	0.765905	0.765715	0.765625
(0.50, 0.25)	1.533480	1.531916	1.531472	1.53125
(0.75, 0.25)	2.300714	2.298296	2.297356	2.296875
(0.25, 0.50)	0.815198	0.813377	0.812794	0.812500
(0.50, 0.50)	1.629552	1.626573	1.625527	1.625000
(0.75, 0.50)	2.443177	2.439522	2.438174	2.437500
(0.25, 0.75)	0.893627	0.891704	0.891000	0.890625
(0.50, 0.75)	1.786779	1.783241	1.781937	1.781250
(0.75, 0.75)	2.678461	2.674354	2.672723	2.671875

Numerical values of T , u_r and u_z at selected interior points are compared with the exact solution of the problem in Tables 1, 2 and 3 respectively. The exact solution is given by

$$T(r, z) = 3r^2 - z^3, \quad u_r(r, z) = 3r + rz^2, \quad u_z(r, z) = 4z - 2r^2.$$

From the tables, it is obvious that the accuracy of the numerical values improves when more boundary elements and interior collocation points are employed in the boundary element calculation.

Table 3. A comparison of the numerical and exact values of u_z at selected interior points.

(r, z)	Set A	Set B	Set C	Exact
(0.25, 0.25)	0.871572	0.874477	0.874852	0.875000
(0.50, 0.25)	0.496347	0.499169	0.499743	0.500000
(0.75, 0.25)	-0.129133	-0.126418	-0.125473	-0.125000
(0.25, 0.50)	1.876029	1.876178	1.875435	1.875000
(0.50, 0.50)	1.500802	1.500796	1.500297	1.500000
(0.75, 0.50)	0.874228	0.874962	0.875001	0.875000
(0.25, 0.75)	2.880382	2.877597	2.875904	2.875000
(0.50, 0.75)	2.505703	2.502466	2.500857	2.500000
(0.75, 0.75)	1.878916	1.876782	1.875625	1.875000

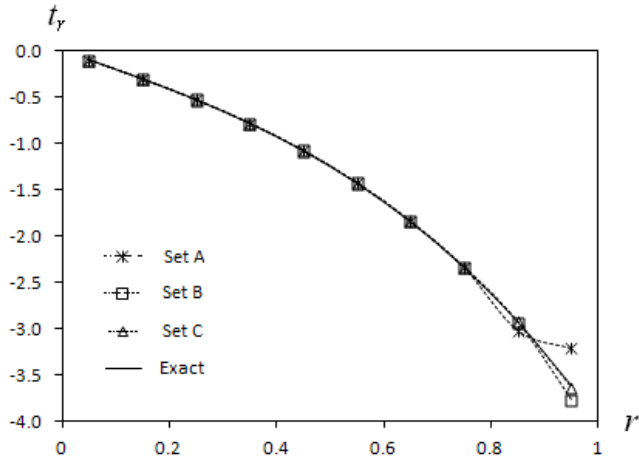


Figure 2. A graphical comparison of the numerical and exact traction component t_r on the boundary $0 < r < 1$, $z = 1$.

In the particular problem under consideration here, the tractions are not known a priori on the boundary. In Figures 2 and 3, the numerically computed traction components t_r and t_z on the boundary $z = 1$ are plotted against r (for $0 < r < 1$) and compared with the values of t_r and t_z calculated from the exact solution of the problem. The numerical values of t_r and t_z from Set A (that is, from the boundary element computation using $(N, L) = (30, 9)$) are rather inaccurate at boundary points very close to the sharp corner point $(r, z) = (1, 1)$. As shown in the plots for Sets B and C, the numerical values of t_r and t_z at boundary points near $(r, z) = (1, 1)$, however, converge to the exact values when more elements and interior collocation points are used in the numerical calculation.

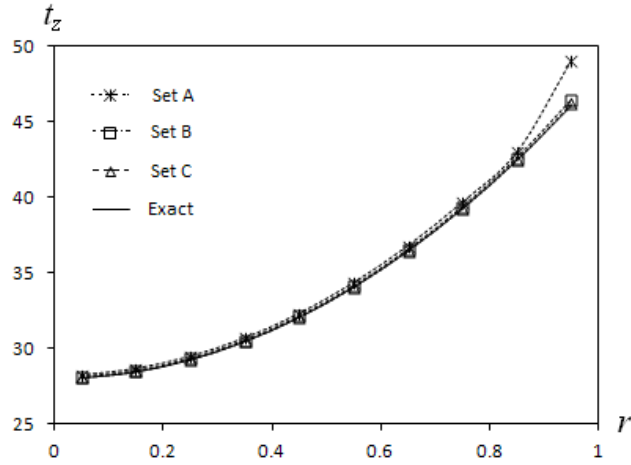


Figure 3. A graphical comparison of the numerical and exact traction component t_z on the boundary $0 < r < 1$, $z = 1$.

Problem 2. Consider a hollow cylindrical solid whose thermoelastic properties are radially graded. More specifically, the solid occupies the region $r_1 < r < r_2$, $0 < z < z_1$, and thermal conductivity κ , the stress-temperature coefficient β , the shear modulus μ , the Poisson's ratio ν are chosen as $\kappa = \kappa_0 r$, $\beta = \beta_0 r$, $\mu = \mu_0 r$ and $\nu = 1/10$ respectively. The reference temperature is taken to be given by $T_0 = 0$ and the internal heat generation and body force terms by $Q(r) = 0$, $F_r(r) = 0$ and $F_z(r) = 0$.

The boundary conditions are given by

$$\left. \begin{aligned} T(r_1, z) &= T_1 \\ T(r_2, z) &= T_2 \\ t_r(r_1, z) &= 0 \\ t_r(r_2, z) &= 0 \\ t_z(r_1, z) &= 0 \\ t_z(r_2, z) &= 0 \end{aligned} \right\} \text{for } 0 < z < z_1$$

and

$$\left. \begin{array}{l} \frac{\partial T}{\partial z} \Big|_{z=0} = 0 \\ \frac{\partial T}{\partial z} \Big|_{z=1} = 0 \\ t_r(r, z_1) = 0 \\ t_r(r, z_2) = 0 \\ u_z(r, z_1) = 0 \\ u_z(r, z_2) = 0 \end{array} \right\} \text{for } r_1 < r < r_2,$$

where T_1 and T_2 are given constants.

The temperature and the other thermoelastic fields vary with r only. The problem may be solved analytically. The exact solution is given by

$$T(r, z) = T_1 + (T_2 - T_1) \frac{(r_1 - r)r_2}{(r_1 - r_2)r},$$

$$\begin{aligned} u_r(r, z) &= C_2 r^{-\frac{1}{2}(1 - \frac{\sqrt{5-14\nu+9\nu^2}}{-1+\nu})} + C_1 r^{-\frac{1}{2}(1 + \frac{\sqrt{5-14\nu+9\nu^2}}{-1+\nu})} \\ &\quad + \frac{r\beta_0(\nu - \frac{1}{2})}{\mu_0} \left(\frac{r_2(T_2 - T_1)}{r_1 - r_2} - T_1 \right), \\ u_z(r, z) &= 0, \end{aligned}$$

where C_1 and C_2 are constants determining by using the boundary conditions $\sigma_{rr}(r_1, z) = 0$ and $\sigma_{rr}(r_2, z) = 0$.

The boundary element solution in Section 6 will be checked here against the exact solution above for the particular case in which $r_1 = 1$, $r_2 = 2$, $z_1 = 1$, $T_1 = 1$, $T_2 = 2$, $\kappa_0 = 1$, $\beta_0 = 1$ and $\mu_0 = 1$. For this particular case, the constants C_1 and C_2 are given by $C_1 = -0.758832$ and $C_2 = 0.256974$.

The boundary Γ consists of four straight lines. For the boundary element solution, each straight line is discretized into N_0 elements, so the total number of element is $N = 4N_0$. The interior collocation points are chosen at point $(1 + i/(L_0 + 1), j/(L_0 + 1))$ for $i, j = 1, 2, \dots, L_0$, therefore, the total number

of interior collocation points is given by $L = L_0^2$. To obtain some numerical results, $N_0 = 40$ and $L_0 = 15$ are used.

Table 4. A comparison of the numerical and exact values of T , u_r and u_z at selected interior points.

(r, z)	Numerical (T, u_r, u_z)	Exact (T, u_r, u_z)
(1.25, 0.25)	(1.39990, 0.82146, 0.00009)	(1.40000, 0.81992, 0)
(1.50, 0.25)	(1.66664, 0.98261, 0.00006)	(1.66667, 0.98108, 0)
(1.75, 0.25)	(1.85717, 1.16617, 0.00004)	(1.85714, 1.16460, 0)
(1.25, 0.50)	(1.39995, 0.82148, 0.00000)	(1.40000, 0.81992, 0)
(1.50, 0.50)	(1.66664, 0.98262, 0.00000)	(1.66667, 0.98108, 0)
(1.75, 0.50)	(1.85715, 1.16618, 0.00000)	(1.85714, 1.16460, 0)
(1.25, 0.75)	(1.39990, 0.82146, -0.00009)	(1.40000, 0.81992, 0)
(1.50, 0.75)	(1.66664, 0.98261, -0.00006)	(1.66667, 0.98108, 0)
(1.75, 0.75)	(1.85717, 1.16617, -0.00004)	(1.85714, 1.16460, 0)

In Table 4, the numerical values of the temperature T and the displacement components u_r and u_z are obtained and compared with the values computed from the exact solution. There is a good agreement between the numerical and exact values.

Figure 4 shows plots of the numerical and the exact temperature against r for $1 < r < 2$ at $z = 0.50$. (Note that the temperature is independent of z .) The two plots for the numerical and the exact temperature are visually almost indistinguishable.

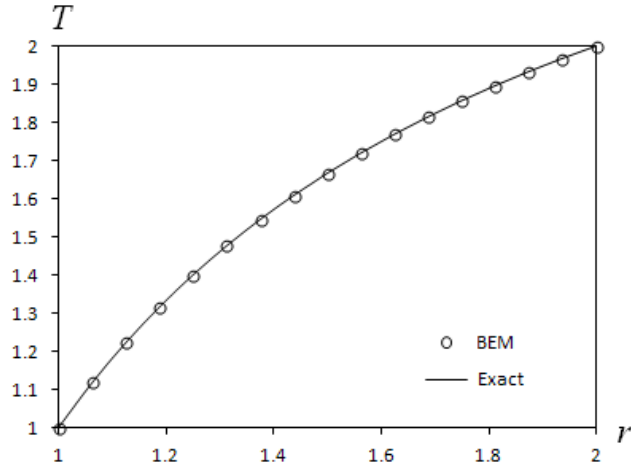


Figure 4. Plots of the numerical and the exact temperature against r for $0 < r < 1$ at $z = 0.50$.

The interior thermoelastic stresses σ_{rr} , σ_{rz} , σ_{zz} and $\sigma_{\theta\theta}$ can be computed numerically using (4) and (33). For the particular problem here, σ_{rz} vanishes throughout the solution domain since the displacement components u_r and u_z are functions of r alone. Plots of the numerically computed and the exact σ_{rr} , σ_{zz} and $\sigma_{\theta\theta}$ against r for $1 < r < 2$ at $z = 0.50$ are given in Figure 5. The numerical and the exact values of the thermoelastic stresses are in good agreement with each other.

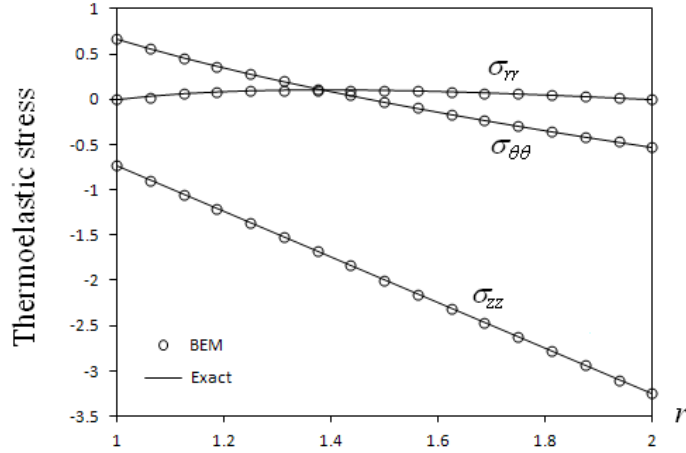


Figure 5. Plots of the numerical and the exact thermoelastic stresses against r for $0 < r < 1$ at $z = 0.50$.

Problem 3. Consider a solid cylinder which occupies the region $0 < r < H, 0 < z < H$, where H is a positive constant. The thermal conductivity, shear modulus and stress-temperature coefficient of the cylinder vary exponentially along the z axis as given respectively by $\kappa = \kappa_0 \exp(-hz)$, $\mu = \mu_0 \exp(-hz)$ and $\beta = \beta_0 \exp(-hz)$, where κ_0, μ_0, β_0 and h are positive constants.

There is no heat generation and body forces in the cylinder, that is, $Q = 0$ and $F_r = F_z = 0$. A uniform heat flux q_0 enters the solid through the part of the boundary where $0 < r < H/2, z = 0$. The end of the cylinder at $z = H$ is maintained at uniform temperature T_0 (that is, the constant reference temperature at which the body does not experience any thermally induced stress) and is attached to a rigid wall (so that $u_r = u_z = 0$ on $0 < r < H, z = h$). The parts of the boundary given by $H/2 < r < H, z = 0$ and $0 < z < H, r = H$ are thermally insulated. Apart from the fixed end at $z = H$, the boundary of the cylinder is free of traction.

For this problem, if $\beta_0 = 0$, the cylinder is undeformed, that is, the deformation of the cylinder is purely due to thermal effects. Taking $\nu = 0.3$, $hH = 0.50$ and $(q_0H)/(\kappa_0T_0) = 0.30$, we examine the effects of varying β_0T_0/μ_0 on the displacements and stresses on different parts of the boundary of the cylinder. For the dual-reciprocity boundary element method, the boundary of the cylinder is discretized into 270 equal length element and 361 well distributed interior collocation points are chosen.

The displacement components u_r and u_z are not known a priori at the end of the cylinder at $z = 0$. In Figures 6 and 7, u_r/H and u_z/H at $z = 0$ are plotted against r/H ($0 < r/H < 1$) for selected values of β_0T_0/μ_0 . From the figures, it is obvious that increasing β_0T_0/μ_0 has the effect of increasing the magnitudes of u_r/H and u_z/H . The effect of β_0T_0/μ_0 on u_r appears to be more pronounced at larger distance from the center $(0, 0)$ of the cylinder while the effect on u_z seems to be greater nearer to $(0, 0)$.

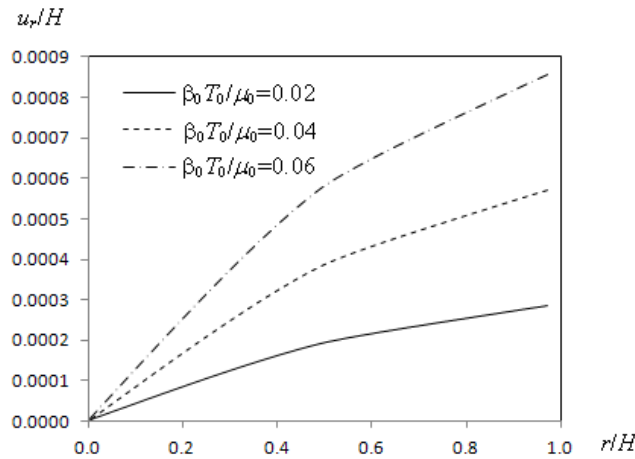


Figure 6. Plots of u_r/H at $z = 0$ against r/H for selected values of β_0T_0/μ_0 .

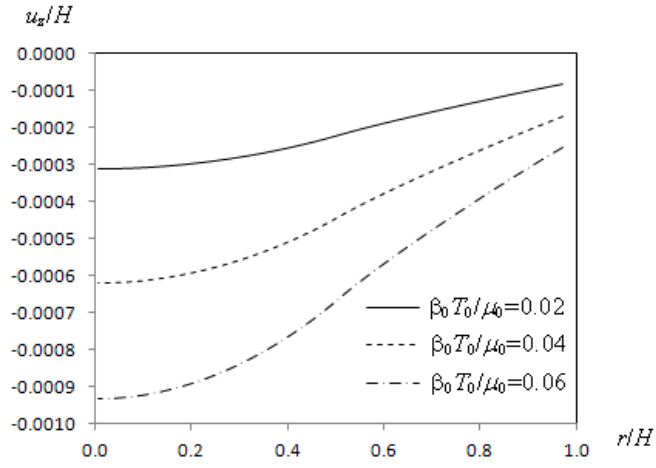


Figure 7. Plots of u_z/H at $z = 0$ against r/H for selected values of $\beta_0 T_0 / \mu_0$.

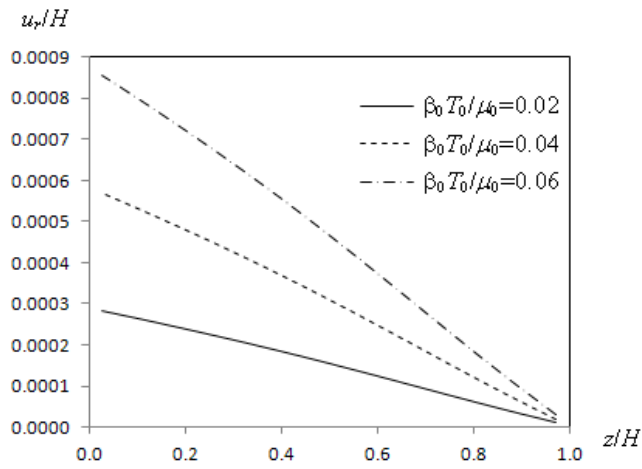


Figure 8. Plots of u_r/H at $r = 1$ against z/H for selected values of $\beta_0 T_0 / \mu_0$.

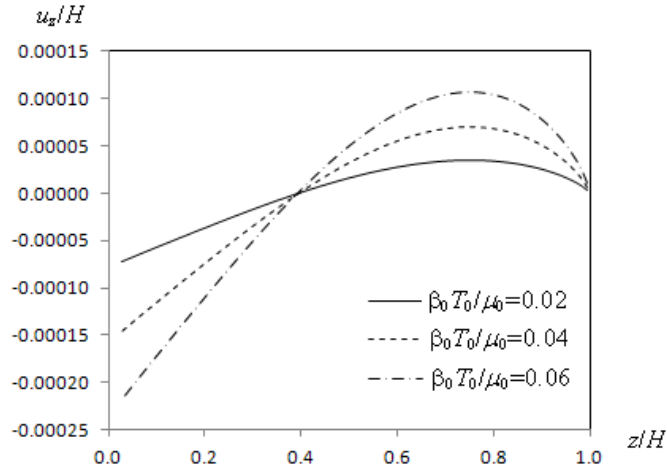


Figure 9. Plots of u_z/H at $r = 1$ against z/H for selected values of $\beta_0 T_0/\mu_0$.

Plots of u_r and u_z on the traction free surface $r = 1$ against z/H ($0 < z/H < 1$) are given in Figures 8 and 9 for selected values of $\beta_0 T_0/\mu_0$. As before, the magnitudes of u_r/H and u_z/H increase with increasing $\beta_0 T_0/\mu_0$. The displacement component u_r decreases in magnitude as z/H increases and the component u_z changes in sign near $z/H = 0.40$. As expected, both components u_r and u_z are extremely small near the fixed end of the cylinder at $z = H$.

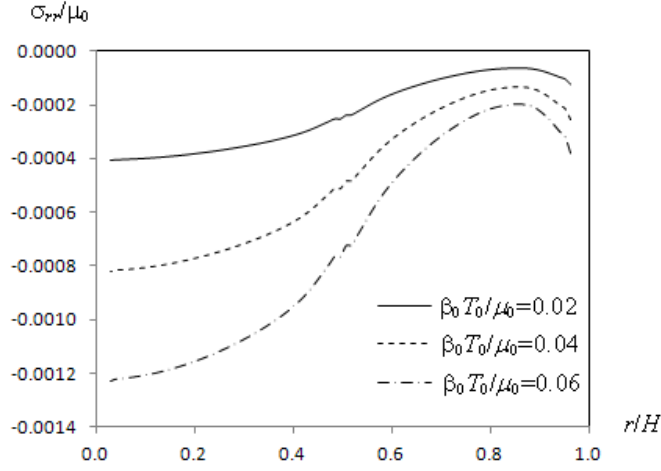


Figure 10. Plots of σ_{rr}/μ_0 on $z/H = 0$ against r/H for selected values of $\beta_0 T_0/\mu_0$.

For selected values of $\beta_0 T_0/\mu_0$, the radial stress σ_{rr}/μ_0 and the hoop stress $\sigma_{\theta\theta}/\mu_0$ on $z/H = 0$ are plotted against r/H ($0 < r/H < 1$) in Figures 10 and 11 respectively, and the longitudinal stress σ_{zz}/μ_0 and the hoop stress $\sigma_{\theta\theta}/\mu_0$ on $r/H = 1$ are plotted against z/H ($0 < z/H < 1$) in Figures 12 and 13 respectively. Increasing $\beta_0 T_0/\mu_0$ appears to increase the magnitudes of the stresses. At the end $z/H = 0$ of the cylinder, the radial stress σ_{rr}/μ_0 has larger magnitude at points nearer to the center where heating occurs. The magnitude of the longitudinal stress σ_{zz}/μ_0 on the cylindrical surface $r/H = 1$ as z/H gets closer to 1, that is, the magnitude of the stress is larger at points nearer to the fixed end of the cylinder.

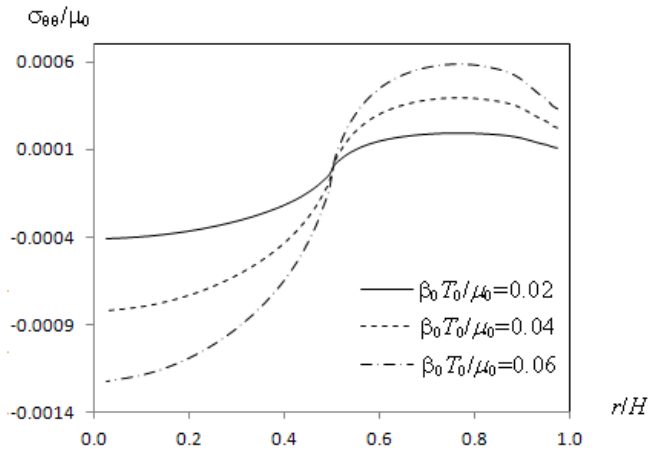


Figure 11. Plots of $\sigma_{\theta\theta}/\mu_0$ on $z/H = 0$ against r/H for selected values of $\beta_0 T_0/\mu_0$.

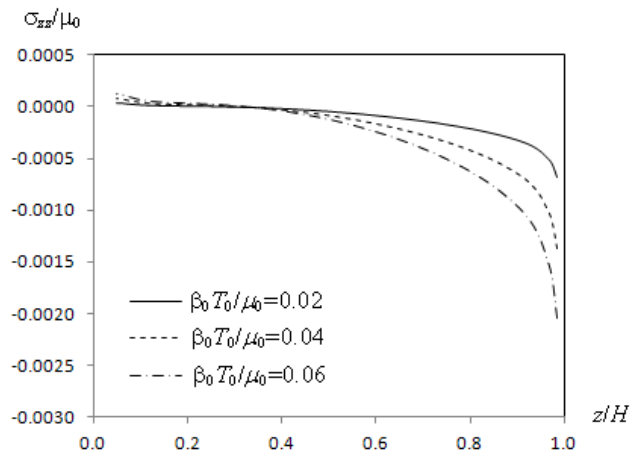


Figure 12. Plots of σ_{zz}/μ_0 on $r/H = 1$ against z/H for selected values of $\beta_0 T_0/\mu_0$.

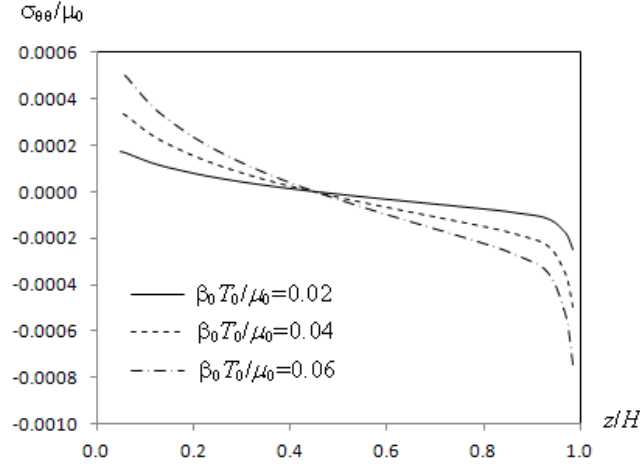


Figure 13. Plots of $\sigma_{\theta\theta}/\mu_0$ on $r/H = 1$ against z/H for selected values of $\beta_0 T_0/\mu_0$.

8 Summary and conclusion

We have implemented a dual-reciprocity boundary element procedure for calculating axisymmetric thermoelastostatic fields in nonhomogeneous solids with material properties that vary continuously from point to point in space. New interpolating functions that are bounded but in relatively simple elementary forms are used in the dual-reciprocity method for treating domain integrals which appear in the integral formulation of the thermoelastic problem under consideration.

Numerical results for specific test problems with known analytical closed-form solutions indicate that the temperature, displacement and stress fields can be accurately computed by the proposed dual-reciprocity boundary element approach.

References

- [1] J. P. Agnantiaris, D. Polyzos and D. E. Beskos, Free vibration analysis of non-axisymmetric and axisymmetric structures by the dual-reciprocity BEM, *Engineering Analysis with Boundary Elements* **25** (2001) 713-723.
- [2] W. T. Ang and D. L. Clements, A boundary element method for determining the effect of holes on the stress distribution around a crack, *International Journal for Numerical Methods in Engineering* **23** (1986) 1727-1737.
- [3] W. T. Ang, D. L. Clements and N. Vahdati, A dual-reciprocity boundary element method for a class of elliptic boundary value problems for nonhomogeneous anisotropic media, *Engineering Analysis with Boundary Elements* **27** (2003) 49-55.
- [4] A. A. Bakr, *The Boundary Integral Equation Method in Axisymmetric Stress Analysis Problems*, Berlin Heidelberg New York Tokyo, Springer-Verlag, 1986.
- [5] C. A. Brebbia and J. Dominguez, Boundary element methods for potential problems, *Applied Mathematical Modelling* **1** (1977) 372-378.
- [6] C. A. Brebbia and D. Nardini, Dynamic analysis in solid mechanics by an alternative boundary element procedure, *International Journal of Soil Dynamics and Earthquake Engineering* **2** (1983) 228-233.
- [7] C. A. Brebbia, J. C. F. Telles and L. C. Wrobel, *Boundary Element Techniques, Theory and Applications in Engineering*, Springer-Verlag, Berlin/Heidelberg, 1984.

- [8] P. K. Chaudhuri and S. Ray, Effects of an axisymmetric rigid punch on a nonhomogeneous transversely isotropic half-space, *ANZIAM Journal* **44** (2003) 461-474.
- [9] D. L. Clements and J. Kusuma, Axisymmetric loading of a class of inhomogeneous transversely isotropic half-spaces with quadratic elastic moduli, *Quarterly Journal of Mechanics and Applied Mathematics* **64** (2011) 25-46.
- [10] T. A. Cruse, D. W. Snow and R. B. Wilson, Numerical solutions in axisymmetric elasticity, *Computers and Structures* **7** (1977) 445-451.
- [11] G. F. Dargush and P. K. Banerjee, Time-dependent axisymmetric thermoelastic boundary element analysis, *International Journal for Numerical Methods in Engineering* **33** (1992) 695-717.
- [12] J. Liang and S. Subramaniam, Computation of molecular electrostatics with boundary element methods, *Biophysical Journal* **73** (1997) 1830-1841.
- [13] A. Mammoli and M. S. Ingber, Stokes flow around cylinder in a bounded two-dimensional domain using multipole accelerated boundary element methods, *International Journal for Numerical Methods in Engineering* **44** (1999) 897-917.
- [14] Y. Ochiai, V. Sladek and J. Sladek, Axial symmetric elasticity analysis in non-homogeneous bodies under gravitational load by triple-reciprocity boundary element method, *International Journal for Numerical Methods in Engineering* **78** (2009) 779-799.

- [15] K. H. Park, A BEM formulation for axisymmetric elasticity with arbitrary body force using particular integrals, *Computers and Structures* **80** (2002) 2507-2514.
- [16] F. J. Rizzo, An integral equation approach to boundary value problems of classical elastostatics, *Quarterly of Applied Mathematics* **25** (1967) 83-95.
- [17] T. J. Rudolphi, Axisymmetric thermoelasticity by combined boundary and finite elements, *Engineering Computations* **5** (1988) 59-64.
- [18] E. E. Theotokoglou and L. H. Stampoulouglou, The radially nonhomogeneous elastic axisymmetric problem, *International Journal of Solids and Structures* **45** (2008) 6535-6552.
- [19] H. C. Wang and P. K. Banerjee, Generalized axisymmetric elastodynamic analysis by boundary element method, *International Journal for Numerical Methods in Engineering* **30** (1990) 115-131.
- [20] L. C. Wrobel and C. A. Brebbia, A formulation of the boundary element method for axisymmetric transient heat conduction, *International Journal of Heat and Mass Transfer* **24** (1981) 843-850.
- [21] B. I. Yun and W. T. Ang, A dual-reciprocity boundary element approach for axisymmetric nonlinear time-dependent heat conduction in a nonhomogeneous solid, *Engineering Analysis with Boundary Elements* **34** (2010) 697-706.

Appendix A

The functions $G_0(\underline{\mathbf{x}}; \underline{\mathbf{x}}_0)$ and $G_1(\underline{\mathbf{x}}; \underline{\mathbf{x}}_0; \underline{\mathbf{n}}(\underline{\mathbf{x}}))$ in (7) are given by

$$G_0(\underline{\mathbf{x}}; \underline{\mathbf{x}}_0) = -\frac{K(m(\underline{\mathbf{x}}; \underline{\mathbf{x}}_0))}{\pi \sqrt{a(\underline{\mathbf{x}}; \underline{\mathbf{x}}_0) + b(r; r_0)}},$$

$$G_1(\underline{\mathbf{x}}; \underline{\mathbf{x}}_0; \underline{\mathbf{n}}(\underline{\mathbf{x}})) = -\frac{1}{\pi \sqrt{a(\underline{\mathbf{x}}; \underline{\mathbf{x}}_0) + b(r; r_0)}} \times \left\{ \frac{n_r(\underline{\mathbf{x}})}{2r} \left[\frac{r_0^2 - r^2 + (z_0 - z)^2}{a(\underline{\mathbf{x}}; \underline{\mathbf{x}}_0) - b(r; r_0)} E(m(\underline{\mathbf{x}}; \underline{\mathbf{x}}_0)) - K(m(\underline{\mathbf{x}}; \underline{\mathbf{x}}_0)) \right] + n_z(\underline{\mathbf{x}}) \frac{z_0 - z}{a(\underline{\mathbf{x}}; \underline{\mathbf{x}}_0) - b(r; r_0)} E(m(\underline{\mathbf{x}}; \underline{\mathbf{x}}_0)) \right\},$$

where $K(m)$ and $E(m)$ being the complete elliptic integrals of the first and second kind respectively and

$$m(\underline{\mathbf{x}}; \underline{\mathbf{x}}_0) = \frac{2b(r; r_0)}{a(\underline{\mathbf{x}}; \underline{\mathbf{x}}_0) + b(r; r_0)},$$

$$a(\underline{\mathbf{x}}; \underline{\mathbf{x}}_0) = r_0^2 + r^2 + (z_0 - z)^2, \quad b(r; r_0) = 2rr_0.$$

Appendix B

The functions $\Phi_{IJ}(\underline{\mathbf{x}}; \underline{\mathbf{x}}_0)$ and $\Psi_{IJ}(\underline{\mathbf{x}}; \underline{\mathbf{x}}_0; \underline{\mathbf{n}}(\underline{\mathbf{x}}))$ in (9) are given by

$$\Phi_{rr}(\underline{\mathbf{x}}; \underline{\mathbf{x}}_0) = \frac{1}{8\pi(1-\nu)r_0 C(\underline{\mathbf{x}}; \underline{\mathbf{x}}_0)} \left\{ ((3-4\nu)(r_0^2 + r^2) + 4(1-\nu)(z_0 - z)^2) K(m(\underline{\mathbf{x}}; \underline{\mathbf{x}}_0)) + (-[C(\underline{\mathbf{x}}; \underline{\mathbf{x}}_0)]^2(3-4\nu) - \frac{(z_0 - z)^2}{D(\underline{\mathbf{x}}; \underline{\mathbf{x}}_0)} A(\underline{\mathbf{x}}; \underline{\mathbf{x}}_0)) E(m(\underline{\mathbf{x}}; \underline{\mathbf{x}}_0)) \right\},$$

$$\Phi_{rz}(\underline{\mathbf{x}}; \underline{\mathbf{x}}_0) = \frac{(z_0 - z)}{8\pi(1-\nu)C(\underline{\mathbf{x}}; \underline{\mathbf{x}}_0)} \left\{ -K(m(\underline{\mathbf{x}}; \underline{\mathbf{x}}_0)) + \frac{B(\underline{\mathbf{x}}; \underline{\mathbf{x}}_0)}{D(\underline{\mathbf{x}}; \underline{\mathbf{x}}_0)} E(m(\underline{\mathbf{x}}; \underline{\mathbf{x}}_0)) \right\},$$

$$\Phi_{zr}(\underline{\mathbf{x}}; \underline{\mathbf{x}}_0) = \frac{r(z_0 - z)}{8\pi(1 - \nu)r_0 C(\underline{\mathbf{x}}; \underline{\mathbf{x}}_0)} \left\{ K(m(\underline{\mathbf{x}}; \underline{\mathbf{x}}_0)) - \frac{A(\underline{\mathbf{x}}; \underline{\mathbf{x}}_0) - 2r_0^2}{D(\underline{\mathbf{x}}; \underline{\mathbf{x}}_0)} E(m(\underline{\mathbf{x}}; \underline{\mathbf{x}}_0)) \right\},$$

$$\Phi_{zz}(\underline{\mathbf{x}}; \underline{\mathbf{x}}_0) = \frac{r}{4\pi(1 - \nu)C(\underline{\mathbf{x}}; \underline{\mathbf{x}}_0)} \left\{ (3 - 4\nu)K(m(\underline{\mathbf{x}}; \underline{\mathbf{x}}_0)) + \frac{(z_0 - z)^2}{D(\underline{\mathbf{x}}; \underline{\mathbf{x}}_0)} E(m(\underline{\mathbf{x}}; \underline{\mathbf{x}}_0)) \right\},$$

$$\Psi_{rr}(\underline{\mathbf{x}}; \underline{\mathbf{x}}_0; \underline{\mathbf{n}}(\underline{\mathbf{x}})) = -\frac{r}{2\pi(1 - \nu)} (\Lambda_1(\underline{\mathbf{x}}; \underline{\mathbf{x}}_0)n_r(\underline{\mathbf{x}}) + \Lambda_2(\underline{\mathbf{x}}; \underline{\mathbf{x}}_0)n_z(\underline{\mathbf{x}})),$$

$$\Psi_{rz}(\underline{\mathbf{x}}; \underline{\mathbf{x}}_0; \underline{\mathbf{n}}(\underline{\mathbf{x}})) = -\frac{r}{2\pi(1 - \nu)} (\Lambda_3(\underline{\mathbf{x}}; \underline{\mathbf{x}}_0)n_r(\underline{\mathbf{x}}) + \Lambda_4(\underline{\mathbf{x}}; \underline{\mathbf{x}}_0)n_z(\underline{\mathbf{x}})),$$

$$\Psi_{zr}(\underline{\mathbf{x}}; \underline{\mathbf{x}}_0; \underline{\mathbf{n}}(\underline{\mathbf{x}})) = -\frac{r}{2\pi(1 - \nu)} (\Lambda_5(\underline{\mathbf{x}}; \underline{\mathbf{x}}_0)n_r(\underline{\mathbf{x}}) + \Lambda_6(\underline{\mathbf{x}}; \underline{\mathbf{x}}_0)n_z(\underline{\mathbf{x}})),$$

$$\Psi_{zz}(\underline{\mathbf{x}}; \underline{\mathbf{x}}_0; \underline{\mathbf{n}}(\underline{\mathbf{x}})) = -\frac{r}{2\pi(1 - \nu)} (\Lambda_7(\underline{\mathbf{x}}; \underline{\mathbf{x}}_0)n_r(\underline{\mathbf{x}}) + \Lambda_8(\underline{\mathbf{x}}; \underline{\mathbf{x}}_0)n_z(\underline{\mathbf{x}})),$$

where $K(m)$ and $E(m)$ being the complete elliptic integrals of the first and second kind respectively and

$$\begin{aligned} \Lambda_1(\underline{\mathbf{x}}; \underline{\mathbf{x}}_0) &= \frac{1}{2r_0r^2C(\underline{\mathbf{x}}; \underline{\mathbf{x}}_0)} \left\{ (1 - 2\nu)(A(\underline{\mathbf{x}}; \underline{\mathbf{x}}_0) + H(\underline{\mathbf{x}}; \underline{\mathbf{x}}_0)) \right. \\ &\quad - \frac{1}{[C(\underline{\mathbf{x}}; \underline{\mathbf{x}}_0)]^2 D(\underline{\mathbf{x}}; \underline{\mathbf{x}}_0)} (-2(z_0 - z)^6 + (-5r_0^2 - 4r^2)(z_0 - z)^4 \\ &\quad \left. + (5r_0^2r^2 - 4r_0^4 - r^4)(z_0 - z)^2 + (r^2 - r_0^2)^3 \right\} K(m(\underline{\mathbf{x}}; \underline{\mathbf{x}}_0)) \\ &\quad + \frac{1}{2r_0r^2C(\underline{\mathbf{x}}; \underline{\mathbf{x}}_0)D(\underline{\mathbf{x}}; \underline{\mathbf{x}}_0)} \left\{ -(1 - 2\nu)(2A(\underline{\mathbf{x}}; \underline{\mathbf{x}}_0)B(\underline{\mathbf{x}}; \underline{\mathbf{x}}_0) \right. \\ &\quad \left. + 3r^2(A(\underline{\mathbf{x}}; \underline{\mathbf{x}}_0) - 2r_0^2)) \right. \\ &\quad + \frac{1}{[C(\underline{\mathbf{x}}; \underline{\mathbf{x}}_0)]^2 D(\underline{\mathbf{x}}; \underline{\mathbf{x}}_0)} (-2(z_0 - z)^8 + (-6r^2 - 7r_0^2)(z_0 - z)^6 \\ &\quad \left. + (-9r_0^4 + 2r_0^2r^2 - 5r^4)(z_0 - z)^4 \right. \\ &\quad \left. + (-5r_0^6 + 10r_0^4r^2 - 5r_0^2r^4)(z_0 - z)^2 \right. \\ &\quad \left. + (-r_0^8 + 2r_0^6r^2 - 2r_0^2r^4 + r^8) \right\} E(m(\underline{\mathbf{x}}; \underline{\mathbf{x}}_0)), \end{aligned}$$

$$\begin{aligned}
\Lambda_2(\underline{\mathbf{x}}; \underline{\mathbf{x}}_0) &= \Lambda_5(\underline{\mathbf{x}}; \underline{\mathbf{x}}_0) = \frac{z_0 - z}{2r_0 r C(\underline{\mathbf{x}}; \underline{\mathbf{x}}_0)} \{(1 - 2\nu) \\
&+ \frac{1}{[C(\underline{\mathbf{x}}; \underline{\mathbf{x}}_0)]^2 D(\underline{\mathbf{x}}; \underline{\mathbf{x}}_0)} ((z_0 - z)^2 (3A(\underline{\mathbf{x}}; \underline{\mathbf{x}}_0) - 2(z_0 - z)^2) \\
&+ 2(r_0^2 - r^2)^2)\} K(m(\underline{\mathbf{x}}; \underline{\mathbf{x}}_0)) \\
&+ \frac{z_0 - z}{2r_0 r C(\underline{\mathbf{x}}; \underline{\mathbf{x}}_0) D(\underline{\mathbf{x}}; \underline{\mathbf{x}}_0)} \{-(1 - 2\nu) A(\underline{\mathbf{x}}; \underline{\mathbf{x}}_0) \\
&- \frac{1}{[C(\underline{\mathbf{x}}; \underline{\mathbf{x}}_0)]^2 D(\underline{\mathbf{x}}; \underline{\mathbf{x}}_0)} ((z_0 - z)^4 (4A(\underline{\mathbf{x}}; \underline{\mathbf{x}}_0) - 3(z_0 - z)^2) \\
&+ (r_0^2 - r^2)^2 (2A(\underline{\mathbf{x}}; \underline{\mathbf{x}}_0) + 3(z_0 - z)^2))\} E(m(\underline{\mathbf{x}}; \underline{\mathbf{x}}_0)),
\end{aligned}$$

$$\begin{aligned}
\Lambda_3(\underline{\mathbf{x}}; \underline{\mathbf{x}}_0) &= -\frac{z_0 - z}{2r^2 [C(\underline{\mathbf{x}}; \underline{\mathbf{x}}_0)]^3 D(\underline{\mathbf{x}}; \underline{\mathbf{x}}_0)} (2r^2 (r^2 - r_0^2 + 2(z_0 - z)^2) \\
&+ A(\underline{\mathbf{x}}; \underline{\mathbf{x}}_0) B(\underline{\mathbf{x}}; \underline{\mathbf{x}}_0)) K(m(\underline{\mathbf{x}}; \underline{\mathbf{x}}_0)) \\
&+ \frac{z_0 - z}{C(\underline{\mathbf{x}}; \underline{\mathbf{x}}_0) D(\underline{\mathbf{x}}; \underline{\mathbf{x}}_0)} \left\{ (1 - 2\nu) - \frac{1}{2r^2 [C(\underline{\mathbf{x}}; \underline{\mathbf{x}}_0)]^2 D(\underline{\mathbf{x}}; \underline{\mathbf{x}}_0)} \right. \\
&\times (-[H(\underline{\mathbf{x}}; \underline{\mathbf{x}}_0)]^3 + r^2 (z_0 - z)^2 (2r_0^2 + r^2 - 5(z_0 - z)^2) \\
&\left. + r^2 (7r_0^4 - 11r_0^2 r^2 + 5r^4) \right\} E(m(\underline{\mathbf{x}}; \underline{\mathbf{x}}_0)),
\end{aligned}$$

$$\begin{aligned}
\Lambda_4(\underline{\mathbf{x}}; \underline{\mathbf{x}}_0) &= \Lambda_7(\underline{\mathbf{x}}; \underline{\mathbf{x}}_0) = \frac{1}{2r C(\underline{\mathbf{x}}; \underline{\mathbf{x}}_0)} \{(1 - 2\nu) \\
&+ \frac{(z_0 - z)^2}{[C(\underline{\mathbf{x}}; \underline{\mathbf{x}}_0)]^2 D(\underline{\mathbf{x}}; \underline{\mathbf{x}}_0)} B(\underline{\mathbf{x}}; \underline{\mathbf{x}}_0)\} K(m(\underline{\mathbf{x}}; \underline{\mathbf{x}}_0)) \\
&+ \frac{1}{2r C(\underline{\mathbf{x}}; \underline{\mathbf{x}}_0) D(\underline{\mathbf{x}}; \underline{\mathbf{x}}_0)} \{-(1 - 2\nu) B(\underline{\mathbf{x}}; \underline{\mathbf{x}}_0) \\
&+ \frac{(z_0 - z)^2}{[C(\underline{\mathbf{x}}; \underline{\mathbf{x}}_0)]^2 D(\underline{\mathbf{x}}; \underline{\mathbf{x}}_0)} (-A(\underline{\mathbf{x}}; \underline{\mathbf{x}}_0) B(\underline{\mathbf{x}}; \underline{\mathbf{x}}_0) \\
&+ 6r^2 (A(\underline{\mathbf{x}}; \underline{\mathbf{x}}_0) - 2r_0^2))\} E(m(\underline{\mathbf{x}}; \underline{\mathbf{x}}_0)),
\end{aligned}$$

$$\begin{aligned}
\Lambda_6(\underline{\mathbf{x}}; \underline{\mathbf{x}}_0) &= \frac{1}{2r_0 C(\underline{\mathbf{x}}; \underline{\mathbf{x}}_0)} \{ (1 - 2\nu) \\
&\quad - \frac{(z_0 - z)^2}{[C(\underline{\mathbf{x}}; \underline{\mathbf{x}}_0)]^2 D(\underline{\mathbf{x}}; \underline{\mathbf{x}}_0)} (A(\underline{\mathbf{x}}; \underline{\mathbf{x}}_0) - 2r_0^2) \} K(m(\underline{\mathbf{x}}; \underline{\mathbf{x}}_0)) \\
&\quad + \frac{1}{2r_0 C(\underline{\mathbf{x}}; \underline{\mathbf{x}}_0) D(\underline{\mathbf{x}}; \underline{\mathbf{x}}_0)} \{ -(1 - 2\nu)(A(\underline{\mathbf{x}}; \underline{\mathbf{x}}_0) - 2r_0^2) \\
&\quad + \frac{(z_0 - z)^2}{[C(\underline{\mathbf{x}}; \underline{\mathbf{x}}_0)]^2 D(\underline{\mathbf{x}}; \underline{\mathbf{x}}_0)} (A(\underline{\mathbf{x}}; \underline{\mathbf{x}}_0)(A(\underline{\mathbf{x}}; \underline{\mathbf{x}}_0) - 2r_0^2) \\
&\quad - 6r_0^2 B(\underline{\mathbf{x}}; \underline{\mathbf{x}}_0)) \} E(m(\underline{\mathbf{x}}; \underline{\mathbf{x}}_0)),
\end{aligned}$$

$$\begin{aligned}
\Lambda_8(\underline{\mathbf{x}}; \underline{\mathbf{x}}_0) &= \frac{(z_0 - z)^3}{[C(\underline{\mathbf{x}}; \underline{\mathbf{x}}_0)]^3 D(\underline{\mathbf{x}}; \underline{\mathbf{x}}_0)} K(m(\underline{\mathbf{x}}; \underline{\mathbf{x}}_0)) + \frac{(z_0 - z)}{C(\underline{\mathbf{x}}; \underline{\mathbf{x}}_0) D(\underline{\mathbf{x}}; \underline{\mathbf{x}}_0)} \\
&\quad \times \{ -(1 - 2\nu) - \frac{4(z_0 - z)^2}{[C(\underline{\mathbf{x}}; \underline{\mathbf{x}}_0)]^2 D(\underline{\mathbf{x}}; \underline{\mathbf{x}}_0)} A(\underline{\mathbf{x}}; \underline{\mathbf{x}}_0) \} E(m(\underline{\mathbf{x}}; \underline{\mathbf{x}}_0)),
\end{aligned}$$

$$A(\underline{\mathbf{x}}; \underline{\mathbf{x}}_0) = r_0^2 + r^2 + (z_0 - z)^2, \quad B(\underline{\mathbf{x}}; \underline{\mathbf{x}}_0) = r_0^2 - r^2 + (z_0 - z)^2,$$

$$C(\underline{\mathbf{x}}; \underline{\mathbf{x}}_0) = \sqrt{(r_0 + r)^2 + (z_0 - z)^2}, \quad D(\underline{\mathbf{x}}; \underline{\mathbf{x}}_0) = (r_0 - r)^2 + (z_0 - z)^2,$$

$$H(\underline{\mathbf{x}}; \underline{\mathbf{x}}_0) = r_0^2 + (z_0 - z)^2.$$

Appendix C

The functions $\phi_{IJ}(\underline{\mathbf{x}}; \underline{\mathbf{y}})$ and $\tau_{IJ}(\underline{\mathbf{x}}; \underline{\mathbf{y}}; \underline{\mathbf{n}}(\underline{\mathbf{x}}))$ constructed using (20), (24) and (25) are given by

$$\begin{aligned}
\phi_{rr}(\underline{\mathbf{x}}; \underline{\mathbf{y}}) &= -\left\{ \left(\frac{4}{3} - \frac{\rho}{3r} \right) \sigma(\underline{\mathbf{x}}; \underline{\mathbf{y}}) + \left(\frac{4}{3} + \frac{\rho}{3r} \right) \sigma(\underline{\mathbf{x}}; -\rho, \zeta) \right. \\
&\quad - \frac{2}{3} (z - z_0)^2 [\sigma(0, z; \underline{\mathbf{y}})]^{-1} - \frac{2}{3} \sigma(0, z; \underline{\mathbf{y}}) \\
&\quad - \frac{1}{9r^2} [[\sigma(\underline{\mathbf{x}}; \underline{\mathbf{y}})]^3 + [\sigma(\underline{\mathbf{x}}; -\rho, \zeta)]^3 - 2[\sigma(0, z; \underline{\mathbf{y}})]^3] \\
&\quad + \frac{1}{1 - 2\nu} \left[\left(\frac{2}{3} - \frac{\rho}{3r} \right) \sigma(\underline{\mathbf{x}}; \underline{\mathbf{y}}) + \left(\frac{2}{3} + \frac{\rho}{3r} \right) \sigma(\underline{\mathbf{x}}; -\rho, \zeta) \right. \\
&\quad + \frac{1}{3} (r - \rho)^2 [\sigma(\underline{\mathbf{x}}; \underline{\mathbf{y}})]^{-1} + \frac{1}{3} (r + \rho)^2 [\sigma(\underline{\mathbf{x}}; -\rho, \zeta)]^{-1} \\
&\quad \left. \left. - \frac{1}{9r^2} [[\sigma(\underline{\mathbf{x}}; \underline{\mathbf{y}})]^3 + [\sigma(\underline{\mathbf{x}}; -\rho, \zeta)]^3 - 2[\sigma(0, z; \underline{\mathbf{y}})]^3] \right\},
\end{aligned}$$

$$\begin{aligned}\phi_{zr}(\underline{\mathbf{x}}; \underline{\mathbf{y}}) &= -\frac{(z-\zeta)}{3(1-2\nu)}\{(r-\rho)[\sigma(\underline{\mathbf{x}}; \underline{\mathbf{y}})]^{-1} + (r+\rho)[\sigma(\underline{\mathbf{x}}; -\rho, \zeta)]^{-1}\} \\ &\quad + \frac{1}{r}[\sigma(\underline{\mathbf{x}}; \underline{\mathbf{y}}) + \sigma(\underline{\mathbf{x}}; -\rho, \zeta) - 2\sigma(0, z; \underline{\mathbf{y}})],\end{aligned}$$

$$\phi_{rz}(\underline{\mathbf{x}}; \underline{\mathbf{y}}) = -\frac{(z-\zeta)}{3(1-2\nu)}\{(r-\rho)[\sigma(\underline{\mathbf{x}}; \underline{\mathbf{y}})]^{-1} + (r+\rho)[\sigma(\underline{\mathbf{x}}; -\rho, \zeta)]^{-1}\},$$

$$\begin{aligned}\phi_{zz}(\underline{\mathbf{x}}; \underline{\mathbf{y}}) &= -\left\{\left(\frac{4}{3} - \frac{\rho}{3r}\right)\sigma(\underline{\mathbf{x}}; \underline{\mathbf{y}}) + \left(\frac{4}{3} + \frac{\rho}{3r}\right)\sigma(\underline{\mathbf{x}}; -\rho, \zeta)\right. \\ &\quad \left. + \frac{1}{3(1-2\nu)}[(z-\zeta)^2[\sigma(\underline{\mathbf{x}}; \underline{\mathbf{y}})]^{-1} + (z-\zeta)^2[\sigma(\underline{\mathbf{x}}; -\rho, \zeta)]^{-1}\right. \\ &\quad \left. + \sigma(\underline{\mathbf{x}}; \underline{\mathbf{y}}) + \sigma(\underline{\mathbf{x}}; -\rho, \zeta)]\right\},\end{aligned}$$

$$\begin{aligned}\tau_{rr}(\underline{\mathbf{x}}; \underline{\mathbf{y}}; \underline{\mathbf{n}}(\underline{\mathbf{x}})) &= 2n_r(\underline{\mathbf{x}})\left\{\frac{1-\nu}{3(1-2\nu)}[(r-\rho)\sigma(\underline{\mathbf{x}}; \underline{\mathbf{y}}) + (r+\rho)\sigma(\underline{\mathbf{x}}; -\rho, \zeta)]\right. \\ &\quad \left. + \frac{\nu}{9(1-2\nu)r}[[\sigma(\underline{\mathbf{x}}; \underline{\mathbf{y}})]^3 + [\sigma(\underline{\mathbf{x}}; -\rho, \zeta)]^3 - 2[\sigma(0, z; \underline{\mathbf{y}})]^3]\right\} \\ &\quad + n_z(\underline{\mathbf{x}})\left\{\frac{(z-\zeta)}{3}[\sigma(\underline{\mathbf{x}}; \underline{\mathbf{y}}) + \sigma(\underline{\mathbf{x}}; -\rho, \zeta) - 2\sigma(0, z; \underline{\mathbf{y}})]\right\},\end{aligned}$$

$$\begin{aligned}\tau_{zr}(\underline{\mathbf{x}}; \underline{\mathbf{y}}; \underline{\mathbf{n}}(\underline{\mathbf{x}})) &= n_r(\underline{\mathbf{x}})\left\{\frac{(z-\zeta)}{3}[\sigma(\underline{\mathbf{x}}; \underline{\mathbf{y}}) + \sigma(\underline{\mathbf{x}}; -\rho, \zeta) - 2\sigma(0, z; \underline{\mathbf{y}})]\right\} \\ &\quad + 2n_z(\underline{\mathbf{x}})\left\{\frac{\nu}{3(1-2\nu)}[(r-\rho)\sigma(\underline{\mathbf{x}}; \underline{\mathbf{y}}) + (r+\rho)\sigma(\underline{\mathbf{x}}; -\rho, \zeta)]\right. \\ &\quad \left. + \frac{\nu}{9(1-2\nu)r}[[\sigma(\underline{\mathbf{x}}; \underline{\mathbf{y}})]^3 + [\sigma(\underline{\mathbf{x}}; -\rho, \zeta)]^3 - 2[\sigma(0, z; \underline{\mathbf{y}})]^3]\right\},\end{aligned}$$

$$\begin{aligned}\tau_{rz}(\underline{\mathbf{x}}; \underline{\mathbf{y}}; \underline{\mathbf{n}}(\underline{\mathbf{x}})) &= \frac{2n_r(\underline{\mathbf{x}})\nu(z-\zeta)}{3(1-2\nu)}[\sigma(\underline{\mathbf{x}}; \underline{\mathbf{y}}) + \sigma(\underline{\mathbf{x}}; -\rho, \zeta)] \\ &\quad + \frac{n_z(\underline{\mathbf{x}})}{3}[(r-\rho)\sigma(\underline{\mathbf{x}}; \underline{\mathbf{y}}) + (r+\rho)\sigma(\underline{\mathbf{x}}; -\rho, \zeta)],\end{aligned}$$

$$\begin{aligned}\tau_{zz}(\underline{\mathbf{x}}; \underline{\mathbf{y}}; \underline{\mathbf{n}}(\underline{\mathbf{x}})) &= \frac{n_r(\underline{\mathbf{x}})}{3}[(r-\rho)\sigma(\underline{\mathbf{x}}; \underline{\mathbf{y}}) + (r+\rho)\sigma(\underline{\mathbf{x}}; -\rho, \zeta)] \\ &\quad + \frac{2n_z(\underline{\mathbf{x}})(1-\nu)(z-\zeta)}{3(1-2\nu)}[\sigma(\underline{\mathbf{x}}; \underline{\mathbf{y}}) + \sigma(\underline{\mathbf{x}}; -\rho, \zeta)].\end{aligned}$$